J Mater Sci (2021) 56:2856–2878

Review

Hydrogen production from ammonia borane hydrolysis catalyzed by non-noble metal-based materials: a review

Chenyang Wang[1], Jianling Zhao[1], Xihua Du[1], Shuo Sun[1], Xiaofei Yu[1], Xinghua Zhang[1], Zunming Lu[1], Lanlan Li[1], and Xiaojing Yang[1,*]

[1] *School of Materials Science and Engineering, Hebei University of Technology, Tianjin 300130, People's Republic of China*

Received: 14 August 2020
Accepted: 21 October 2020
Published online:
3 November 2020

ABSTRACT

As a promising chemical hydrogen storage material, ammonia borane (AB, NH_3BH_3) has been receiving significant attention for its hydrogen release property. Researches on the development of effective catalysts for AB hydrolysis under mild conditions have been of potential application interest. In the last few years, some non-noble metal-based materials have been developed for dehydrogenation of AB via hydrolysis, due to their low cost, high activity, and high durability. Therefore, the summary and analysis of the rapidly developing non-noble metal catalyst systems without noble metals can better grasp the current development status to guide subsequent design and research. In this review, the latest advances in non-noble metal-based catalysts are summarized, which can be divided into the following categories: pure metal-based materials, metal-based compounds (borides, phosphides, and oxides), and metal/metal compound heterogeneous structures. Investigations into the composition, structure, and activity enhancement of the catalyst are further highlighted. Besides, hydrolysis mechanisms, catalyst persistence, and AB regeneration are also discussed.

Handling Editor: Christopher Blanford.

Address correspondence to E-mail: yangxiaojing@hebut.edu.cn

https://doi.org/10.1007/s10853-020-05493-7

GRAPHICAL ABSTRACT

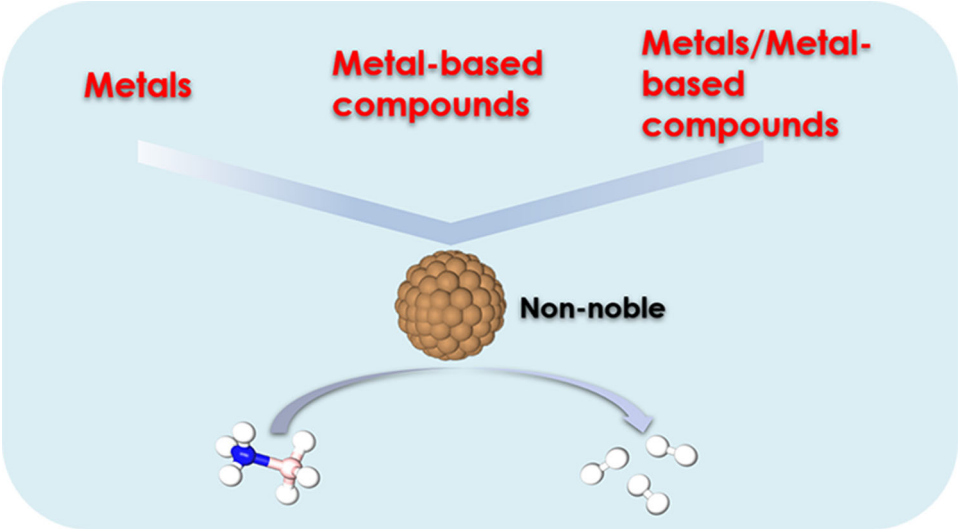

Abbreviations

AB	Ammonia borane, NH_3BH_3
ALD	Atomic layer deposition
CNTs	Carbon nanotubes
DFT	Density functional theory
e^-/h^+	Electrons and holes
EXAFS	Extended X-ray absorption fine structure
FT	Fourier transform
GO	Graphene oxide
HGR	Hydrogen generation rate
KIEs	Kinetic isotope effects
LSPRs	Localized surface plasmon resonances
MOFs	Metal-organic frameworks
NCs	Nanoclusters
NCN	Nitric acid-treated carbon nitride
NFs	Nanofibers
NTs	Nanotubes
NPs	Nanoparticles
·OH	Hydroxyl radicals
PCC	Porous coordination cages
PEI	Polyethyleneimine
RDS	Rate-determining step
rGO	Reduced graphene oxide
SSA	Specific surface area
THF	Tetrahydrofuran
TOF	Turnover frequency
UV–Vis	Ultraviolet–visible
XAS	X-ray absorption spectroscopy
XPS	X-ray photoelectron spectroscopy
3D	Three-dimensional

Introduction

Nowadays, global energy demand is increasing dramatically; nonetheless, the problems associated with scarcity of fossil energy and environmental pollution have been unable to meet the requirements of human development [1–3]. Recently, attention has been turned toward the development and utilization of new energy sources, such as wind, tidal, and nuclear energy, to sustain energy demand. Hydrogen energy, as a new energy carrier, is considered to be one of the effective substitutes for fossil fuels. Hydrogen has the advantages of rich reserves, high energy density, and zero emissions, thus making it the globally accepted cleanest energy carrier [4, 5]. However, difficult storage, requirement of efficient transportation methods of hydrogen, and controlled release of hydrogen limit the development and utilization of hydrogen energy.

Compared to the currently used high-pressure and low-temperature liquid hydrogen storage technologies, hydrogen storage materials with higher hydrogen content can better meet the requirements of mobile applications due to their stability and light weight [6, 7]. Although porous materials (e.g., carbon materials, metal–organic frameworks (MOFs), and organic complexes) can physically adsorb hydrogen through weak van der Waals forces at extremely low operating temperatures to form hydrogen storage materials, they are not conducive to practical applications [8, 9]. In contrast, chemical hydrogen storage materials (hydrogen storage alloys, light metal hydrides, B–N hydrides, etc.) usually have a bulk hydrogen density that exceeds that of liquid hydrogen and high hydrogen release purity, thus making them very promising as hydrogen source for fuel cells [5, 10].

Ammonia borane (NH_3BH_3, AB) is the simplest type of B–N hydride, with a molecular weight of only 30.7 g mol^{-1} and a hydrogen storage capacity of up to 19.6 wt.%. Moreover, AB is non-toxic, stable, and environmentally friendly, making it a highly promising candidate for hydrogen storage [11]. At present, AB mainly releases hydrogen in the following two ways: pyrolysis and hydrolysis. Pyrolysis involves the opening of the B–H and N–H bonds in the AB molecule through high temperature, and then the H atoms recombine with each other to release hydrogen. However, this process requires higher temperature (to completely release three equivalents of hydrogen, temperature of above 1200 °C is required), consumes large energy, and generates gaseous by-products which reduce hydrogen purity [12]. Therefore, milder hydrolysis of AB is a more promising way to produce hydrogen. In the hydrolysis reaction, the proton H in water reacts with the ionic H connected to the B atom in AB to release three equivalents of hydrogen, and the hydrogen production is 8.9 wt.% of the raw materials AB and H_2O [13]. The reaction equation is represented as follows:

$$NH_3BH_3 + 2H_2O \rightarrow NH_4^+ + BO_2^- + 3H_2$$

AB can exist stably in water; therefore, the hydrolysis reaction requires the involvement of a suitable catalyst to be carried out under ambient conditions.

Noble metal-based catalysts (Pt, Rh, and Ru) were found to have excellent catalytic activity for the hydrolysis of AB [14–17]. However, due to the high cost and limited resources of noble metals, their practical application is greatly limited. Researchers found that non-noble metals such as Fe, Co, and Ni also show catalytic activity toward hydrolysis of AB [18–20]. Compared to noble metals, the non-noble metals offer reduced cost and higher earth abundance. Besides, non-noble metals are abundant in the types of compounds that can serve as potential catalysts. Although many studies proved that using non-noble metals as dopants or for formation of alloys or heterostructures with noble metals can improve the catalytic activity of the catalyst; nonetheless, the cost of catalysts still remains high [21–28]. The non-noble metal has a much lower catalytic activity than the noble metal, and its problems of easy agglomeration and oxidation are also harmful for efficient catalytic activity. Therefore, improving the activity and durability of the non-noble metal-based catalyst is the focus of current research. So far, significant progress has been made in this field.

Status and development of hydrolysis of AB catalyzed with noble metals have been summarized [29]. At the same time, the research on non-noble metal-based catalysts for catalytic hydrolysis of AB has been developing rapidly, and many types of catalysts have emerged. Moreover, the catalytic activity of non-noble metal-based catalysts has been catching up with that of noble metal-based catalysts. Therefore, it is important to summarize the current research status of non-noble metal-based catalysts, which can guide future researchers. In this review, we intend to summarize the research progress of non-noble metal-based catalysts for the hydrolysis of AB to hydrogen, in the past five years. Research on non-noble metals has focused on the following three types of materials: pure non-noble metal-based materials, non-noble metal-based compounds, and their composite catalysts. This review mainly includes a summary of the catalyst composition, structure, and activity improvement. Furthermore, the advantages and challenges of non-noble metal-based catalysts for the hydrolysis of AB to produce hydrogen are discussed to cope with their future development.

Non-noble metal-based catalyst

Metal

Single metal

Initially, in 2006, inspired by the catalytic activity of noble metals, Xu et al. found that Co and Mo could

also catalyze the hydrolysis of AB, and additionally, supported Co, Ni, and Cu also exhibited excellent catalytic activity [30, 31]. Subsequently, more designs were carried out for pure metal-based catalysts, microstructure design, ligand stabilization, and addition of support to obtain more active sites of the metal to enhance the catalytic activity. In recent years, in addition to the use of $NaBH_4$ or $LiBH_4$ to reduce metal salts, single metal component catalysts could also be obtained by other methods. For instance, Nozaki et al. used amorphous alloys to prepare skeletal Ni and Cu, respectively [32, 33]. The higher specific surface area (SSA) of the skeletal structure catalyst allowed the reactants to be in more contact. The activity of the catalyst thus improved, and reduction in catalytic activity was not observed even after three cycles of use. Fang et al. encapsulated ultra-small Co nanoclusters in soluble porous coordination cages (Co NCs@PCC), wherein the particles size of Co NCs was only 2.5 nm and PCC could very well stabilize and disperse Co NCs [34]. This design could obtain small-sized metals and solve the problem of the ligand covering the active sites. Therefore, the turnover frequency (TOF) value of catalytic hydrolysis of Co NCs@PCC was 90.1 min^{-1}, which could reach the level of noble metals.

Currently, various support materials are used to fabricate well-dispersed metal nanoparticles (NPs), which can control size and dispersion of these NPs. The strong metal–support interactions also make an important reason for the increased activity. A certain degree of electron transfer occurs between the metal and the support; therefore, the active metal components have a more optimized electronic structure. This metal obtains a more optimal adsorption capacity and aggressiveness to the reactants and intermediates, thereby enhancing the activity of the catalyst. Carbon supports (activated carbon, graphene, and carbon nanotubes (CNTs)) are most concerned catalyst candidates [35–39]. Zhang et al. used atomic layer deposition to uniformly disperse Ni on CNTs, and Ni/CNTs showed excellent hydrolysis activity [39]. Zhang et al. used porous carbon prepared by direct carbonization of Co/Zn-MOFs to support Co NPs (Co-HPC), wherein the Co particle size was only 12.1 ± 4.8 nm [40]. Carbon supports prepared with MOFs exhibited a higher SSA, thus making them more conducive to dispersion of metals, and could more effectively contact with the reactants during catalysis. Besides, the initial activity of Co-HPC was still largely maintained after the catalyst was reused 12 times, indicating its good durability. Zhang et al. prepared a highly nitrogen-doped and uniformly embedded Co-based mesoporous carbon (Co@NMC) catalyst with a high SSA (1044 m^2 g^{-1}) [41]. Extended X-ray absorption fine structure (EXAFS) and X-ray photoelectron spectroscopy (XPS) were used to characterize the surface compositions and chemical states of Co@NMC, indicating the decrease in the valence electrons of the Co, and the presence of the strong Co-Nx effect and the Mott–Schottky effect. The Co NPs were stably fixed on the support, showing excellent catalytic activity for hydrolysis. For the modification of the support, Li's group reported a three-dimensional (3D) structure composed of polyethyleneimine (PEI) and graphene oxide (GO) as support of Co NPs [42]. It was found that the spatial distribution and surface-active sites of Co could be controlled. Owing to the stability of the 3D structure and the synergy between the amine group and Co NPs, the Co/PEI-GO exhibited high AB hydrolysis activity and cycle durability.

The high SSA and adjustable pore size of the MOFs can make the NPs have better dispersibility and more number of exposed active sites, thus making them efficient supports [43, 44]. For example, Wang et al. used ZIF-8 to highly disperse Ni NPs with a particle size of only 2.7 nm, which showed excellent catalytic activity (TOF = 85.7 min^{-1}). Besides, according to the kinetic isotope effects (KIEs) design experiment, it was proved that the rate-determining step (RDS) of the hydrolysis reaction was the cleavage of the O–H bond in H_2O [19]. Furthermore, Liu et al. used MIL-101 as a support to study the catalytic activity of Co NPs in amorphous and crystalline phases with different sizes for AB hydrolysis (Fig. 1). The results showed that the amorphous Co/MIL-101 catalyst with small size (1.6–2.6 nm) showed the best performance, the TOF value could reach 51.4 min^{-1}, and the activity did not decrease significantly even after 30 cycles [45].

Semiconductor materials with unique light response characteristics are also used as supports. On the one hand, semiconductor materials can interact with metals by electron transport [46]; on the other hand, these materials can use light energy, and the excited state of photogenerated electrons and holes (e^-/h^+) on the reactants is more conducive to the hydrolysis reaction [47–49]. The post-modified C_3N_4-supported Co NPs exhibited excellent catalytic activity toward hydrolysis of AB under visible light

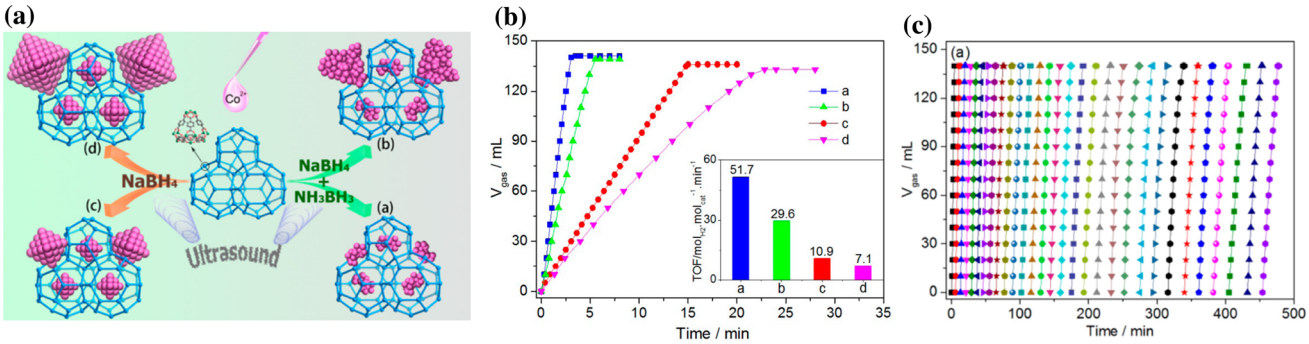

Figure 1 Schematic illustration for the synthesis of four types of MIL-101-supported Co NPs (**a**) and plots of time versus volume of generated H_2 from AB aqueous solution over catalyst (**b**): (a) Co/MIL-101-1-U; (b) Co/MIL-101-1; (c) Co/MIL-101-2-U; (d) Co/MIL-101-2. Inset: corresponding TOF values of the catalysts. Long-time durability characterization of Co/MIL-101–1-U for the generation of H_2 from AB aqueous solution (**c**). Reproduced with permission from ref [45]. Copyright 2017 American Chemical Society.

irradiation [50]. The modified C_3N_4 showed an increased SSA and extended light absorption. The enhanced e^-/h^+ separation of C_3N_4-supported Co NPs efficiency ensures an electron transfer process under light irradiation, leads to an increase in the electron density of Co NPs, and thus improves the catalytic efficiency. Song et al. synthesized a series of porous two-dimensional V_2O_5 nanosheets with oxygen vacancies loaded with Co NPs and performed catalytic hydrolysis under visible light [51]. The band structure of porous V_2O_5 nanosheets with specific oxygen vacancies became controllable, leading to a higher separation of e^-/h^+ than the original V_2O_5. The separated h^+ easily reacted with H_2O molecules to generate hydroxyl radicals (·OH). Besides, the electron density of Co NPs in Co/V_2O_5 increased, indicating the interaction between the metal and support. ·OH and the electrons enriched in Co could favorably attack AB to produce hydrogen. Furthermore, this group also prepared C_3N_4 nanosheet-supported Co and Ni NPs for catalytic hydrogen generation, which showed excellent catalytic activity, with the TOF value of Co-based catalysts reaching 123.2 min^{-1} under visible light irradiation [52]. Besides, BN, SiO_2, and Al_2O_3 have also been used to support metal NPs, and their catalytic activity was found to be excellent. Although some supports cannot optimize the electronic structure of the metal, the stable structure of the support can fix the metal to make it more dispersed and stable. Table 1 summarizes the literature results of metal-based catalysts for AB hydrolysis.

Bi- and multi-metallic

However, the catalytic activity of a single metal is finite. For the first time, in 2009, Xu et al. in situ synthesized FeNi alloy for AB hydrolysis. The prepared nanoalloys possessed Pt-like high catalytic activity [53]. Later studies have shown that the bi- or multi-metallic composite catalyst through component regulation allows the regulation of the electronic structure of catalyst due to the synergistic effect among the different metals, thus providing the optimized activity of the catalyst [54–56]. Zhang et al. prepared Cu@Ni cubic-cage microstructure formed by coating a fine Cu cube with Ni nanospheres. The XPS characterization confirmed that the electrons were transferred from Cu to Ni, and the increase in Cu content facilitated the transfer of more charges to Ni [57]. The synergistic effect between the metal components resulted in an increase in the number of active sites on the catalyst surface. Our previous study explored the relationship between the electronic structure and the catalytic activity of different Co-based alloys toward hydrolysis of AB [58]. The result indicated that the hydrogen production rate of the alloy exhibited a volcanic trend with the center of the d-band, which could affect the absorption of water and AB molecules when the electronic structure was appropriate to obtain excellent activity.

Although synergistic interaction occurs between metals to regulate the electronic structure, some metal elements also as dopants can act as atomic diffusion layers and hinder grain growth. For

Table 1 Summary of the catalytic performance of different pure non-noble metal-based materials for the hydrolysis of AB

Catalyst	Temp (°C)	Light	HGR (mL min^{-1} g^{-1})	TOF (min^{-1})	Ea (kJ/mol)	Refs.
Skeletal Ni	30	–	-	5.3	-	[32]
Co NCs@PCC	25	–	-	90.1	-	[34]
Co@rGO	25	–	-	12.14	45.49	[35]
Co/HPC	50	–	-	2.95	32.8	[40]
Co/CTF	25	–	-	42.3	42.7	[38]
Co/NC	25	–	-	7.6	44.9	[65]
Ni/Ketjen black	25	–	-	7.465	-	[36]
Ni/CNTs	25	–	-	26.2	32.3	[39]
Co@NMC	25	–	-	-	41.6 ± 2	[41]
Co/PEI-GO	25	–	-	18.5	27.4	[42]
Co@N–C-700	25	–	-	5.6	31	[66]
Co/KIT-6	25	–	-	20.05	32.6	[67]
Ni/MIL-101	25	Vis	-	53.97	-	[43]
Co/MIL-101	25	–	-	51.4	31.3	[45]
Co/g-C_3N_4	25	Vis	-	93.8	-	[50]
Ni/g-C_3N_4	25	Vis	-	18.7	36	[68]
Co/C_3N_4 nanosheets	25	Vis	-	123.2	-	[52]
Co/V_2O_5	25	Vis	-	120.4	-	[51]
Ni@h-BN	25	–	-	4.1	47.3	[69]
Ni/BN sheet	25	–	-	1.247	63.2	[70]
Cu/h-BN	25	–	-	0.317	23.8	[71]
Co@TiO_2	25	–	2775	-	26.03	[72]
Cu-ZrO_2	25	–	-	0.384	22.34	[73]
Co/TiC	50	–	-	39.9	36.9	[74]
Co@N–C/SiO_2	25	–	-	8.4	36.1	[75]
CuMo NPs	25	–	-	14.9	51	[54]
NiMo NPs	25	–	-	27.2	32.1	[55]
CuNi-MOFs	30	–	-	40.85 (M)	28.99	[76]
Cu@MoCo	25	–	-	49.61	22.2	[59]
Cu@Ni cubic cage	25	–	14,980	-	40.53	[57]
CoCu NPs	25	–	2179	3.4	33.7	[60]
CuNi NPs	25	–	-	3.54	36.9	[61]
CoNi/HPC	50	–	-	27.22	34.076	[77]
NiFe@CN-G	25	–	-	23.25	38.24	[78]
PVA-CoMo@GO	25	–	-	16.29	43.72	[79]
NiCr/CNFs	25	–	-	5.78	37.6	[80]
FeCo/NCNTs	25	–	-	102	19.89	[18]
CuCo/rGO	25	–	-	50.6	-	[81]
CoW/rGO	25	–	-	16.4	30.7	[82]
CoNi/XC-72	50	–	-	49	28.9	[83]
CoNi/MCNTs	50	–	-	128	52.1	[84]
CuCo/PDA-rGO	30	–	-	51.5 ± 3.7	54.89	[85]
NiMo/graphene	25	–	-	66.7	21.8	[86]
NiCo-GO	25	–	-	6.78	-	[87]
CoCu/C	25	–	-	28.67	51.9	[62]
CuNiCo@MIL-101	25	–	-	72.1	29.1	[88]
CuNi/TiO_2-CdS	25	Vis	9513.51	25.9	32.8	[63]
CuNi/TiO_2(B) NTs	25	Vis	5763.86	15.90	36.14	[47]
CuNi/TiO_2 NFs	25	Vis	8131.15	21.87	27.40	[48]
CuCo/g-C_3N_4	25	Vis	-	75.1	-	[89]
CoNi/Al_2O_3	25	–	-	34.5	32.9	[90]

Table 1 continued

Catalyst	Temp (°C)	Light	HGR (mL min^{-1} g^{-1})	TOF (min^{-1})	Ea (kJ/mol)	Refs.
CuCo/BNNFs	25	–	3387.1	8.42	21.8	[64]
NiCu/SiO_2	25	–	-	25.27	-	[91]
CoCu/Ni foam	25	–	-	30.5	20.8	[92]
CuCo/PDDA-HNTs	25	–	-	30.8	35.15	[93]
CoNi@h-BN	20	–	176.19	–	28	[94]

instance, Wang et al. reported that Cu@MoCo catalysts exhibited significantly higher activity than CuCo catalysts [59]. On the one hand, the addition of Mo could reduce the size of NPs and lead to an increase in active sites; on the other hand, Mo acted as an electron donor, and the synergy between the metal components effectively optimized the electronic structure of the catalyst, thereby reducing the potential barrier of the hydrolysis reaction. In order to overcome the problem of easy agglomeration of metal particles, Sang et al. used dendritic CoCu and NiCu catalysts synthesized with starch, and their catalytic activity was much higher than that of the catalyst without starch [60]. The oleylamine-dispersed CuNi NPs catalyst also showed the effect of enhancing activity [61]. These special dispersants can stabilize metal particles and expose more active sites, which improves metal utilization.

Similarly, the support is advantageous for the dispersion of bi- and multi-metallic catalysts. Bimetallic CuCo alloy NPs supported on activated carbon (CoCu/C) were reported by Bulut et al. [62]. The size of alloy NPs was only 1.8 nm, which resulted in significant increase in its active site. The catalyst showed TOF value of up to 28.67 min^{-1} and good recycling performance (> 95% activity after 10 cycles). Our group also successively studied CuNi alloy NPs supported on TiO_2-based materials, including TiO_2(B) NTs, TiO_2(B)/anatase nanofibers (NFs), and TiO_2-CdS [47, 48, 63]. The stabilization of the support made the metal NPs smaller in size and resulted in their better dispersion. The synergy between Cu and Ni makes the catalyst much more efficient than single metal. Besides, the improvement of the support through these studies makes the catalyst's absorption of light to expand the visible light region, and the utilization efficiency becomes higher. All these effects endow the catalyst with higher hydrolysis activity. This series of work provides better ideas for the conversion of light energy to hydrogen energy. Yang et al. studied CuCo/BN NFs to catalyze the activity of AB. A series of first-principle calculations of the catalyst showed that when the CuCo/BN catalyst adsorbs AB molecules (Fig. 2), the interaction between B and N atoms increases, while the bond length is shortened, indicating that adsorption can inhibit the B–N bond from breaking. Moreover, the B–H bond becomes longer, which is conducive to the release of hydrogen [64]. This also shows the beneficial effect of the synergy between the bimetals toward the hydrolysis reaction. Additional studies on bi- and multi-metallic catalytic hydrolysis are listed in Table 1 for activity comparison. Most bi- and multi- metallic catalysts exhibit significantly improved catalytic activity compared to single metals and to a certain extent reduces the use of specific metal components, which is more conducive to long-term development.

Thus, the above-mentioned description indicates that the current enhancement strategies for non-noble metal-based catalysts are mainly divided into the following four aspects (Fig. 3): multi-component, micromorphology control, caped ligands, and added support. This can provide a certain reference for the design of the non-noble catalysts in the future.

Metal-based compounds

Metal borides

Among metal borides, cobalt boride (Co–B) was first widely studied in 1953 as a catalyst for the hydrogen production reaction via $NaBH_4$ hydrolysis [95]. Co–B has also been used in subsequent studies to catalyze the hydrolysis of AB. Owing to its high catalytic activity, its preparation and catalytic performance have been extensively studied and reported. Wang et al. synthesized a cotton-like CoB alloy (CoB_{ssR}) catalyst through a novel room-temperature solid-state reaction. CoB_{ssR} acquired a large SSA (222.4 m^2 g^{-1})

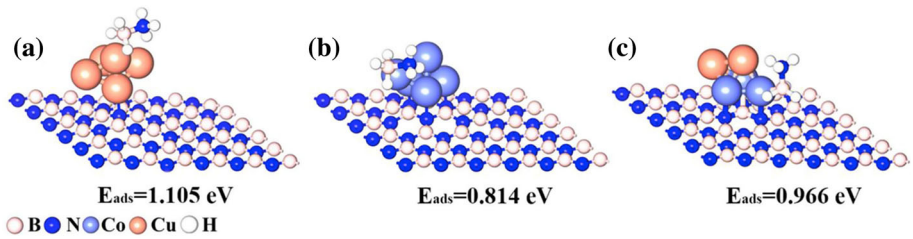

Bond	Pristine AB	AB adsorbed on Cu/h-BN	AB adsorbed on Co/h-BN	AB adsorbed on $Cu_{0.4}Co_{0.6}$/h-BN
B-N	1.658	1.625	1.630	1.623
B-H	1.220	1.256	1.262	1.263
N-H	1.024	1.045	1.045	1.054

Figure 2 The geometrically optimized most stable adsorption structures for AB on Cu/h-BN (**a**), Co/h-BN (**b**), and CuCo/h-BN (**c**), the bond lengths (Å) of adsorbed AB and pristine AB are also indicated. Reproduced with permission from ref [64]. Copyright 2019 Elsevier.

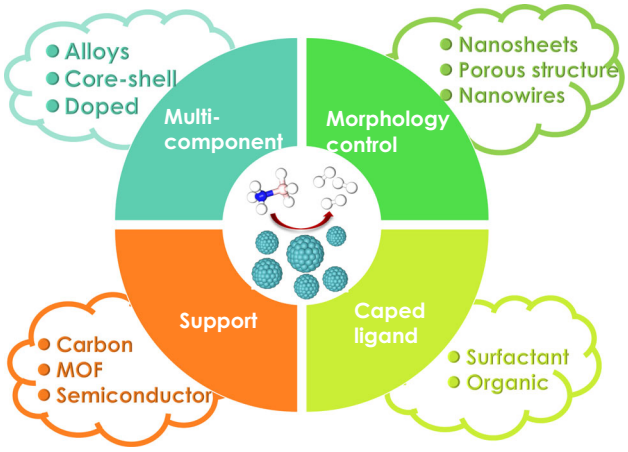

Figure 3 Strategies for enhancing the activity of non-noble metal catalysts and corresponding examples.

and a rich porous structure, making its TOF value twice that of conventional CoB alloys with good durability [96]. CoB films have been investigated for catalytic hydrolysis of AB as they prevent aggregation to a certain extent and have better stability compared to powders [97]. Use of binary transition metal boride is also an important strategy to improve catalytic activity [98].

The substrate stabilizes the catalyst, and the doped elements improve the electronic structure so that the catalytic activity gets enhanced. Based on the research on Co–B thin films, Wang's group synthesized improved Co–B thin-film catalysts doped with Mo or W on different substrates (Ni foam, foam sponge, and Cu foil) [99–102]. Men et al. doped P element into CoB to synthesize CoBP NPs supported on 3D nitrogen-doped graphene hydrogel (CoBP/NGH). Owing to the electron transfer among Co, B, and P and the metal–support interaction, the electrons on Co are enriched, which is beneficial to attacking AB molecules. The hydrolysis of AB obtained by CoBP/NGH showed excellent catalytic performance (TOF = 32.8 min^{-1}), which was better than that of most Co–B-based catalysts reported [103]. However, compared to other types of catalysts (Table 2), the activity of metal borides used for the hydrolysis of AB was still at a relatively low level.

Metal phosphides

Transition metal phosphides (such as Ni_2P and CoP) exhibit the catalytic behavior similar to that of noble metals due to their similar d electron state density. Moreover, metal phosphides are inexpensive; thus, they have been extensively studied in the hydrolysis of AB [104]. In terms of microstructure regulation, CoP and Ni_2P nanosheet arrays prepared by Tang et al. were studied to have the advantages of easy separation and good stability [105, 106].

Many researchers have found that the appropriate concentration of NaOH significantly enhances the activity of the catalyst; nonetheless, the effect of OH^- on the catalyst has not been clearly studied [19, 107]. Fu et al. studied the effect of CoP NPs on the induction period of AB hydrolysis in the presence of anions (OH^-, F^-, and Cl^-). They found that OH^- was the most obvious to reduce the induction period of hydrolysis reaction [108]. Characterization of the electronic structure by XPS indicated that in the absence of anions, CoP exhibited the electrons transfer from Co to P, forming electron-rich $P^{\delta-}$ and electron-deficient $Co^{\delta+}$, which is consistent with the results provided by other researchers. The OH^-

Table 2 Summary of the catalytic performance of different non-noble metal boride/phosphide/oxide-based materials for the hydrolysis of AB

Catalyst	Temp (°C)	HGR (mL min^{-1} g^{-1})	TOF (min^{-1})	Ea (kJ/mol)	Refs.
Co-B NFls/TiO_2 NFs	25	2745.6	–	16.54	[139]
CoB_{SSR}	25	6900	–	22.78	[96]
Co–B thin film	25	5500.0	–	37.8	[97]
CoWB/foam sponge	25	3327.7	–	32.2	[99]
CoMoB/foam sponge	25	5100.0	–	41.7	[100]
CoMoB/Ni foam	25	5331.0	–	45.5	[102]
CoMoB/Cu foil	25	5818.0	–	59.3	[101]
Co-Cr-B/γ-Al_2O_3	25	3260	–	56.06	[140]
Co–Ni-B/PAC	25	1451.2	–	30.2	[98]
Co-Mo-B/Ni foam	25	6027.1	–	43.6	[141]
CoBP/NGH	25	–	32.8	39.4	[103]
CoP	25	–	72.2	-	[108]
Ni_5P_4	25	–	23.5	39	[142]
CoP NA/Ti	25	–	42.8	34.1	[105]
Ni_2P NA/NF	25	–	42.3	44.0	[106]
NiP/rGO	25	–	13.3	34.7	[143]
Ni–P H-Oct/rGO	25	–	34.2 ± 0.6	40.8	[144]
CoP@CNF	25	–	165.5(Co)	48.5	[145]
Ni_2P/C	25	–	13.5	43.4	[146]
CoP/HPC	25	–	27.7	42.55	[147]
CoFeP	60	8915	-	25 ± 3	[148]
NiCoP	25	–	58.4	43.2	[109]
NiFeP/Ni foam	30	7000	-	42.0	[149]
CoNiP/rGo	25	–	18.6	25	[150]
NiCoP@h-BN	25	–	86.5	40.26	[151]
NiCoP/OPC	25	–	95.24	38.9	[107]
CuO	45	294	-	49.2	[113]
CuO–NiO/Co_3O_4	25	–	79.1	23.7	[116]
Cu_2O-CoO	25	–	34.1	20.5	[117]
CoO_x@C/rGo	25	5521(Co)	–	40.57	[115]
CuNiO NPs	60	10,560	–	38.12	[112]
Belt-like NiCuO	25	–	33.43	19.63	[119]
CuCoO/GO	25	–	70.0(M)	45.53	[120]
CuCoO/rGO	25	–	81.7(M)	45.26	[121]
NiCoO-NCN	25	–	76.1(M)	29.33	[122]
$CuCo_2O_4$	25	–	73.4	-	[124]
$CuCo_2O_4$/Ti	25	–	44	23.6	[125]
$MnCo_2O_4$/Ti	25	–	24.3	17.5	[126]
$NiCo_2O_4$/Ti	25	–	50.1	17.5	[127]
$Cu_{0.5}Ni_{0.5}Co_2O_4$	25	–	80.2	28.4	[130]
$Cu_{0.4}Ni_{0.6}Co_2O_4$ NWs	25	–	119.5	33.91	[128]
$Co_xCu_{1-x}Co_2O_4$@$Co_yCu_{1-y}Co_2O_4$	25	–	81.8	24.97	[129]
MoO_3-doped $MnCo_2O_4$	25	–	26.4	34.24	[133]
Mo-doped $CuNiCo_2O_4$	25	–	195.25	–	[132]
$Co_{0.8}Cu_{0.2}MoO_4$	25	–	55.0	39.6	[134]
$Cu_{0.4}Co_{0.6}MoO_4$/g-C_3N_4	25	–	75.7	14.46	[135]
Co_3O_4/$CuMoO_4$	25	–	129.15	23.2	[131]

coordinated with the catalyst, the valence electrons of metallic Co increased, and different valence electron states changed, indicating that the introduction of OH^- on the surface improved the electronic properties of the catalyst. Density functional theory (DFT) calculation of OH^- adsorption on the surface of CoP further proved that the interaction between the metal center and the anion leads to the enrichment of the charge in the CoP, thus enhancing the catalytic activity. This study explains the enhanced catalytic reaction of OH^- and metal phosphides mainly due to the fact that the increase of valence electrons of metal ions is supported by experimental and theoretical calculations.

Similar to previously mentioned metals and metal borides, use of binary metal phosphides also constitutes an effective strategy to enhance catalytic activity. Incorporation of the second metal into the phosphide can optimize the electronic structure and enhance the interaction between the catalyst and the reactants. Hou et al. changed the ratio of Ni/Co in $Ni_{2-x}Co_xP$ catalysts and studied the changes in electronic structures (Figs. 4a–c) [109]. Characterization by XPS and X-ray absorption spectroscopy (XAS) revealed that with the incorporation of Co, the electrons were transferred from the metal to the P center, and change was observed in the coordination structure of the Ni and Co. The phase-shift-free Fourier transform (FT) also showed that Co was successfully doped into the lattice of Ni_2P and partially occupied the initial position of Ni atoms, forming Co–P bonds. The DFT calculation of the electronic structure of $Ni_{2-x}Co_xP$ confirmed that the electron transfer from the metal center to the P center was conducive to the strong adsorption of AB molecules. Therefore, the catalyst could attack the B–N bond more effectively and reduce the reaction barrier. These results also indicate that the incorporation of the second metal element has an enhanced effect on the electronic structure and catalytic activity of the material. NiCoP/GO nanohybrid material was also used in AB hydrolysis catalysis with TOF values of up to 153.9 min^{-1}, even higher than those of noble metal catalysts.

TiO_2 is a good electron-accepting metal oxide. Wang et al. used NiCoP as a sensitizer to design a solar sensitization system, which constituted the state of electron imbalance on the surface of NiCoP/TiO_2 and produced hydrogen by photocatalytic hydrolysis of AB [110]. NiCoP showed wide light absorption over the entire ultraviolet–visible (UV–Vis) range, ensuring full use of visible light by the catalyst.

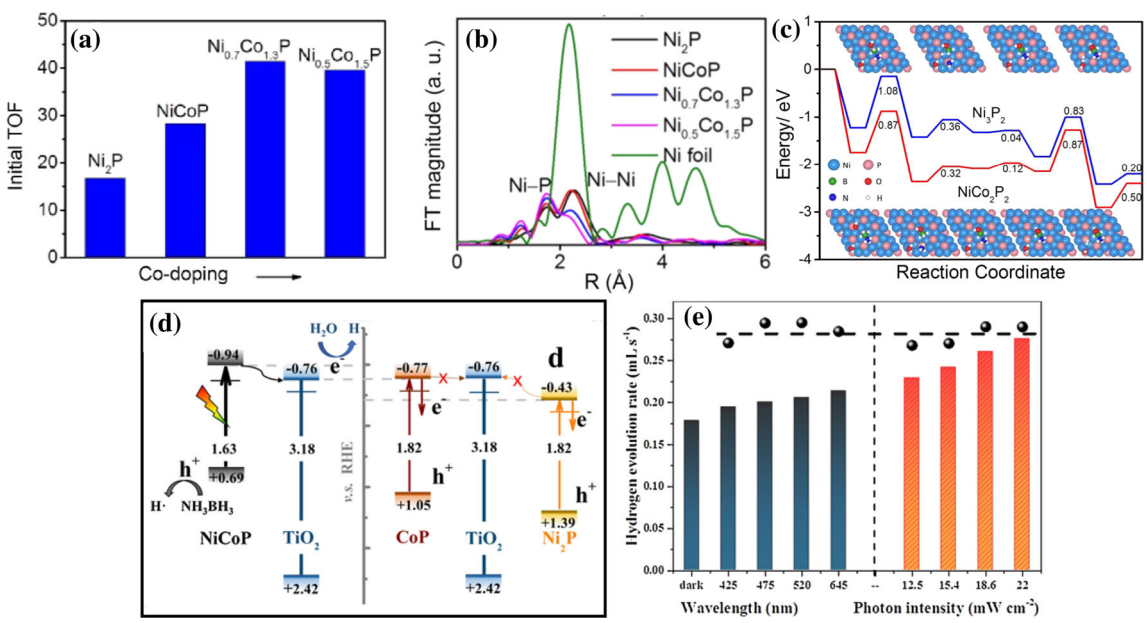

Figure 4 The total TOF values (**a**) and the corresponding FT curves of a series of catalyst (**b**). Energy profiles of AB hydrolytic dehydrogenation on Ni_3P_2(0001) and $NiCo_2P_2$(0001) surfaces with the same initial hydroxyl concentration (**c**). Reproduced with permission from ref [109]. Copyright 2017 the Royal Society of Chemistry. Band structure of phosphides and TiO2 (**d**), and AB hydrogen evolution rate of NiCoP/TiO2 under different light (**e**). Reproduced with permission from ref [110]. Copyright 2020 Elsevier.

Furthermore, the band position of the catalyst was roughly estimated by UV–Vis diffuse absorption spectra (Figs. 4d and e). Unlike traditional photocatalytic water splitting, photogenerated electrons during the reaction do not directly participate in the redox reaction, but rather induce a highly imbalanced charge on NiCoP. The difference in surface charge can significantly promote the activation of B–H and O–H bonds, leading to an increase in the rate of hydrogen release. This study provides new insights and evidence for the mechanism of photocatalytic hydrolysis of AB and indicates that excellent hydrolysis activity is more conducive to the design of subsequent catalysts. Furthermore, other metal phosphides show excellent catalytic activity in the hydrolysis reaction, which are listed in Table 2.

Metal oxides

It is well known that the problem of easy oxidation of transition metals seriously reduces their activity and stability. Although the use of boride and phosphide solves this problem to some extent, the oxidation of transition metals inevitably occurs in these catalysts, which causes a slight decrease in catalytic activity. In 2008, Kalidindi et al. carried out Cu-catalyzed AB hydrolysis and found that Cu_2O was catalytically active, and it was proposed that the reduction of Cu_2O–Cu(0) was due to the release of H_2 facilitated by the attack of water on a transient Cu–H [111]. Some specific non-noble metal oxides, such as Co, Cu, CuCo, NiCo, and CuFe oxides, have been reported to have good catalytic activity [112–118]; thus, more research is conducted in this regard.

The microstructure has an important influence on the catalytic performance. For example, Li et al. studied NiCuO with different micromorphologies to catalyze AB and found that the bracelet-like $Ni_{0.4}Cu_{0.6}O$ nanoplate exhibited the best catalytic activity, with a TOF value of 33.43 min^{-1}. CuO and NiO showed a good synergistic effect in the hydrolysis process [119]. The support was introduced into the catalytic system, and the interaction between the oxide and the support provided powerful help for the catalysis. Feng et al. prepared the hybrids of $Cu_xCo_{1-x}O$ NPs on GO. The optimized hybrid ($Cu_xCo_{1-x}O$/GO) showed superior catalytic performance in the hydrolysis of AB [120]. XAS characterization revealed that the interfacial interaction between CuO-GO was weaker than that in CoO-GO; however, CoO-GO exhibited no catalytic activity during catalysis; thus, it was shown that the addition of Co element could enhance the bonding ability, leading to the enhancement in the interaction between the active component and the support. A new hybrid electronic state was formed in this interaction, which could help improve the catalytic process, thereby enhancing the performance of $Cu_xCo_{1x}O$/GO in AB hydrolysis. This group also studied the cubic CuCoO nanostructures supported on the reduced GO (rGO) based on the study on $Cu_xCo_{1-x}O$/GO [121]. The Cu in the catalyst can activate H_2O and then cooperate with Co to anchor the AB molecule. The interaction between the metal and support results in a high activity of $Cu_{0.5}Co_{0.5}O$/rGO. Furthermore, the conversion of the oxidized state to the metallic state in the catalyst after recycling was studied. The cubic structure of the oxide was broken and the catalyst activity was not restored, a phenomenon that further illustrates the peculiarities of metal oxides. Besides, Feng's group also expanded this research to study $Ni_{0.5}Co_{0.5}O$ NPs hybrid material on nitric acid-treated carbon nitride for the hydrolysis of AB [122].

Inspired by the high performance of oxides in supercapacitors [123], Li and his group developed a series of MCo_2O_4 (M=Cu, Mn, Ni) catalysts for AB hydrolysis [124–127]. Li et al. compared the catalytic activity of $CuCo_2O_4$ catalyst with three different micromorphologies: nanoplates, nanosheets, and unsupported NPs. Among them, $CuCo_2O_4$ nanoplates/Ti showed the best catalytic activity compared to the other two catalytic systems (Fig. 5) [125]. On the one hand, the presence of the Ti substrate can prevent the loss of activity caused by the aggregation of the nanofilm; thus, the catalyst can still maintain 95% of the original activity after eight cycles. On the other hand, the special morphology is expected to have more edges and corners in contrast to the spherical NPs, which can provide more active sites for the catalytic reaction. Besides, the oxidized Co and Cu ions were reduced to metallic Co and Cu after the catalytic reaction. The synergistic effect between Cu and Co could effectively improve the catalytic performance toward hydrolytic dehydrogenation of AB, leading to the TOF value of up to 44 min^{-1}. Similarly, in the study of the catalytic performance of $CuCo_2O_4$ nanoplates, Li's group also proposed that the interaction between the reduced metal state and the support $CuCo_2O_4$ played a positive role in improving the catalytic activity [124]. This group also conducted

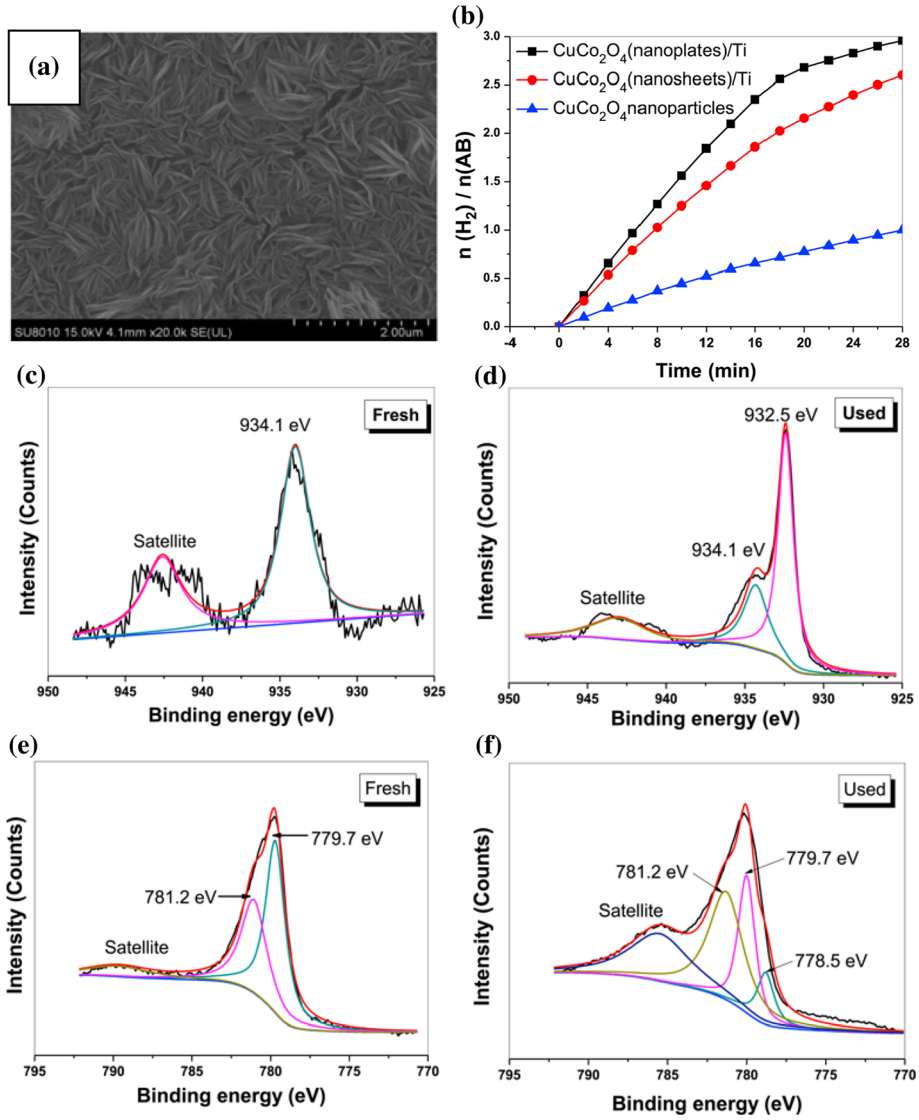

Figure 5 SEM image of $CuCo_2O_4$(nanoplates)/Ti (**a**). The hydrogen evolution when different $CuCo_2O_4$ catalysts were used (**b**). XPS spectra of $CuCo_2O_4$(nanoplates)/Ti: Cu ($2p_{3/2}$) for the fresh and used catalyst (**c–d**), Co ($2p_{3/2}$) for the fresh and used catalyst (**e–f**). Reproduced with permission from ref [125]. Copyright 2017 Elsevier.

extensive research on the introduction of the second transition metal such as Cu, Ni, or Co in the MCo_2O_4 catalyst [128–130]. The synergistic effect of the metal elements in the oxide was found to be beneficial to enhancing the catalytic activity, which is generally superior to that of the single metal component MCo_2O_4, and their TOF values are listed in Table 2. Besides, Mo^{6+} has Lewis acid characteristic, which is beneficial to the adsorption of ·OH; thus, it can enhance the hydrolysis process. Furthermore, extensive research efforts have also been devoted to the study on the incorporation of Mo into the catalyst, and these metal oxide catalysts exhibited superior hydrolytic activity [131–135]. Many of these studies on oxide believe that the reduced metal is the hydrolytic active component, and the remaining oxide serves as the support. Although the metal component has high activity, the interaction between the metal and support is an excellent activity to provide assurance. However, the studies still lack the verification of this interaction, which undeniably requires further research efforts.

MoO_3 has the characteristic of localized surface plasmon resonances (LSPRS); thus, it was used by researchers as a catalyst for AB hydrolysis [136–138]. Yin et al. synthesized MoO_{3-x} structure with a relatively high SSA (30 $m^2\ g^{-1}$) and strong LSPRS in the visible light region. Under visible light irradiation, the catalytic activity of the MoO_{3-x} was much higher than that of commercial MoO_3 for hydrolysis of AB [137]. In addition to the strong LSPRS, MoO_{3-x} forms a new

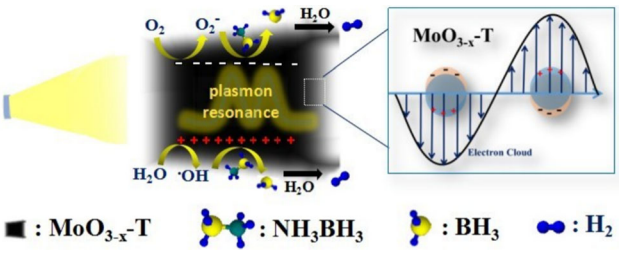

Figure 6 Proposed reaction mechanism of hydrolysis of aqueous AB solution over plasmonic MoO_{3-x} under visible light. Reproduced with permission from ref [137]. Copyright 2017 the Royal Society of Chemistry.

band at the bottom of the original conduction band due to the presence of Mo^{5+} center and oxygen vacancies; thereby, the recombination of e^- and h^+ gets reduced. During the hydrolysis reaction, e^- accumulated on the surface of the catalyst reacts with dissolved O_2 to generate O_2^-, and h^+ reacts with absorbed H_2O to generate ·OH. Subsequently, these groups and H_2O attack MoO_{3-x}-AB complex species to dissociate the B–N bond in AB to form BH_3, thereby leading to the enhancement in the hydrolysis process (Fig. 6). Based on this research, Yin's group incorporated WO_3 into the MoO_{3-x} structure to obtain a stronger LSPRS and optimized its catalytic activity [136]. However, in the study on the photocatalytic hydrolysis of AB, researchers have different views on the mechanism of e^-/h^+ on the catalytic reaction; thus, this topic is worth exploring in future research.

Composite materials of metals and metal-based compounds

Both metals and some specific metal-based compounds have the activity of catalyzing AB. Many studies have found that the interaction between the two active components is very beneficial to the improvement of catalytic activity. For example, Lin et al. designed a carbon-supported Ni/Ni_2P hybrid system [152]. A strong interaction was observed between NPs and carbon in the hybrid system, and electron transfer occurred from Ni to P, which was characterized by XAFS and XPS. P not only caused the surface disorder of NPs, but also changed the chemical environment of Ni in C-Ni/Ni_2P. DFT calculations further indicated that Ni/Ni_2P hybrid system showed higher adsorption energy and lower dissociation energy for H_2O molecules than metal Ni. Besides, carbon-supported Ni NPs could facilitate desorption of ·H in the catalytic H_2 evolution process. The different AB hydrolysis performance obtained by adjusting the hybrid structure of Ni/Ni_2P ratio was more illustrative of the synergistic effect among C, Ni, and Ni/Ni_2P, which promoted the hydrolysis process at the same time.

Li et al. designed a hybrid nanocatalyst composed of metal Cu, $CuCoO_x$, and GO support ($Cu@CuCoO_x@GO$) to promote the room temperature hydrolysis of AB [153]. The $CuCoO_x$ in the catalyst promoted the adsorption of ·OH. At the same time, surface of the Cu metal showed an electron-rich region, which was kinetically favorable to the decomposition of H–OH to ·H. The conductive GO not only dispersed $Cu@CuCoO_x$ to expose more catalytically active sites, but also contributed to electron and substance transfer during the hydrolysis process. These advantages in $Cu@CuCoO_x@GO$ synergistically improved the room temperature catalytic performance toward hydrolysis of AB. Zhang et al. prepared Co–N-doped carbon spherical particles with MOFs as the precursor and then controlled the oxidation to synthesize Co-CoO_x@NCS catalysts of

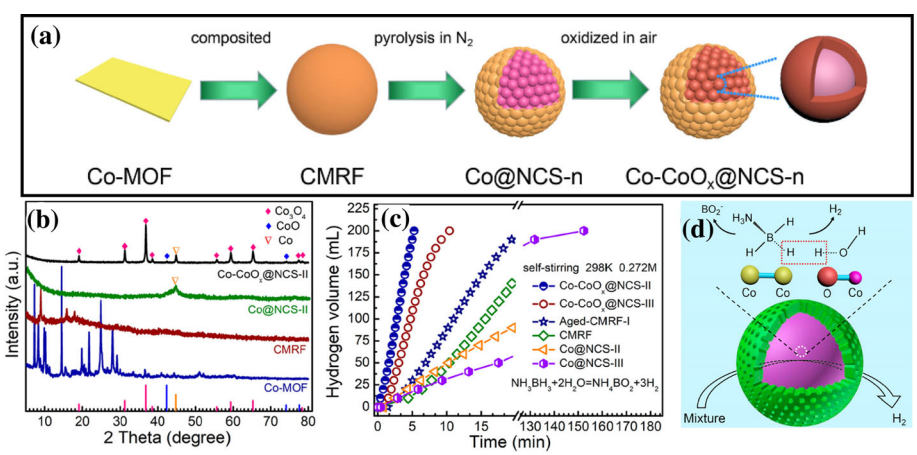

Figure 7 Structural evolution of Co@NCS and Co-CoO_x@NCS (**a**). XRD patterns of various catalysts (**b**). Hydrogen generation catalyzed by various catalysts (**c**). Catalytic mechanism in the reaction system for hydrogen generation of AB (**d**). Reproduced with permission from ref [154]. Copyright 2019 American Chemical Society.

Table 3 Summary of the catalytic performance of different non-noble composite materials of metals and metal-based compounds for the hydrolysis of AB

Catalyst	Temp (°C)	HGR (mL min^{-1} g^{-1})	TOF (min^{-1})	Ea (kJ/mol)	Ref
Ni/Ni_2P	20	-	68.3	44.99	[152]
$Cu@CuCoO_x@GO$	25	-	98.2(M)	35.4	[153]
$Co\text{-}CoO_x@NCS$	25	5562(Co)	-	46.37	[154]
$Cu@Cu_2O$	25	-	13.2	-	[155]
$Ni\text{-}CeO_x$/Graphene	25	-	68.2	28.9	[156]
$Co\text{-}CeO_x$/NGH	25	-	79.5	31.8	[157]

the "birdcage" model (Fig. 7) [154]. Co–CoO_x NPs are surrounded by a porous carbon shell. During the hydrolysis reaction, AB molecules interact with the core NPs. The Co–Co bond activates the B–H bond in AB, and the Co–O bond activates the H–O bond in H_2O; thus, two activated H atoms produce a H_2 molecule. Novel active sites for higher activity in catalytic reactions can be provided by synergistic interactions between metallic Co and CoO_x, and recombination of electronic orbitals between various oxidation-state Co species. Noteworthy, carbon shell limits the growth, aggregation, and loss of active components, while the diffusion of reactants and products can still be conducted through it. The coordination of the entire system makes the catalyst acquire higher reactivity. Besides, $Cu@Cu_2O$ [155], $Ni\text{-}CeO_x$/graphene [156], and $Co\text{-}CeO_x$/NGH [157] have also been studied as AB hydrolysis catalysts (Table 3).

Advantages and challenges

The hydrogen production process of hydrolyzing AB significantly reduces the energy consumption compared to pyrolysis and comparatively can be carried out under extremely milder conditions. Researches on hydrolysis catalysts in recent years have shown that non-noble metal-based catalysts can obtain excellent catalytic activity at a lower cost. Non-noble metal catalysts that can reach the activity level of noble metals lay the foundation for the sustainable development of hydrogen energy. These advantages are shown in Fig. 8, although there are still several problems related to AB hydrolysis.

Recently, the mechanism of the catalyst catalyzing the hydrolysis of AB has been proposed. (1) Similar to the mechanism of $NaBH_4$ hydrolysis, the M–H intermediate is proposed as an important step in the AB hydrolysis reaction [16, 111]. AB molecules are adsorbed on the surface of the catalyst, the H of B–H bond and the metal form an activated intermediate M–H, and then H_2O molecules attack the intermediate. The ·H produced by M–H combines with the ·H produced by H_2O molecules to generate H_2. Therefore, the formation of the M–H intermediate has a great influence on the rate of hydrolysis. (2) Attack of H_2O molecules on the B–N bond in the AB molecule is an important step [120, 158, 159]. First, the reactant molecules are adsorbed on the catalyst surface. When they are in proximity, the O and H atoms in the H_2O molecule are close to the B and N atoms in AB, respectively, thus attacking the B–N bond to make it grow and break to form the transition state B···O and N···H_2. The second H_2O molecule continues to be adsorbed on the surface of the catalyst and attacks -BH_3. The ·H on the BH_3 combines with the ·H in the H_2O molecule to form H_2 and escapes. (3) The

Figure 8 Advantages and challenges in the field of hydrogen production by hydrolysis of ammonia borane.

breaking of the O–H bond in the H_2O molecule is the RDS of the hydrolysis reaction [19, 38, 109]. In terms of experiments, the researchers used the KIE to prove that the bond which breaks in the hydrolysis reaction corresponds to the RDS of the reaction. The ·OH generated after the breaking of the O–H bond in the H_2O molecule can attack the BH_3 group to form a BH_3OH· intermediate, and then ·H is generated, which combines with the ·H generated from the H_2O to eventually form H_2. Most recent researches can only detect and prove a certain step or intermediate of the hydrolysis process through experimental [38] and theoretical simulation calculations [160], but they cannot accurately provide comprehensive understanding of the entire hydrolysis process. Therefore, a more comprehensive study on the mechanism of the catalyst catalyzing the hydrolysis of AB is required.

Nowadays, the durability of the catalyst is also an important issue for AB catalytic hydrolysis. Although the durability of non-noble metal-based catalysts has been significantly improved through numerous research efforts, most of the current studies only evaluate the catalytic activity of catalysts that can be reused within 10 times. However, in practical applications, it is more desirable for the catalyst to have long-lasting usability in order to reduce the waste of resources, thus making it a challenge task in future research.

Besides, the regeneration strategy after AB hydrolysis is still a major issue. Borate is the main product after the hydrolysis reaction and is very stable. The B–O bond in the by-product is very strong, and it is difficult to convert it into a B–H bond; as a result, expensive strong reducing agents are usually required. Ramachandran et al. regenerated AB from the by-product $NH_4B(OMe)_4$ by methanolysis in tetrahydrofuran (THF); $LiAlH_4$ was required as a reducing agent [161]. Liu and his group converted H_3BO_3 into $B(OCH_3)_3$ through methanol esterification and then reacted with NaH to form $NaBH_4$. Then ammonia sulfate reacted with $NaBH_4$ in THF to obtain AB [162]. Regeneration of AB was inseparable from $NaBH_4$ and other hydrogen storage materials, which resulted in increased cost. Besides, regeneration process required a complex process and a large amount of energy. Despite great efforts, the realization of large-scale regeneration of spent fuel still faces major challenges.

Summary and outlook

In this review, recent developments in the use of non-noble metal-based material catalysts for the hydrolysis of AB are summarized. Furthermore, the great improvements made in pure non-noble metal-based materials, metal-based compounds (borides, phosphides, and oxides), and metal/metal-based heterogeneous structural materials, have been discussed. Pure metal-based catalysts are based on the original structure, with significantly improved activity and durability due to microstructural regulation, metal component regulation, and support modification. Therefore, the problem of exposing more active sites to metals and preventing their oxidation and agglomeration is the focus of subsequent research. For the development of metal compounds, non-noble metal-based materials for hydrolysis of AB have been diversified and the consumption of metal resources has been reduced. Metal borides enhance the active surface area, and doping leads to enhancement in activity as indicated by several studies. Metal phosphides and oxides have been receiving increasing attention in recent years for their excellent activity and stability. The heterogeneous structure of metals and metal-based compounds has received significant attention due to their unique internal structure interactions that provide superior capabilities. First, various chemical states of non-noble metals can synergistically enhance the performance of the catalyst. Second, the wide range of compound types offers more possibilities for non-noble metals, which can be exploited for further research. As a whole, non-noble metal-based catalysts have proven to be economical, efficient, and stable catalysts that can be favorable substitutes for noble metals.

Although the catalyst has excellent performance, the study provides more insights into the mechanism of hydrolysis. However, the impact of catalysts on the overall hydrolysis process is not yet known. Moreover, the durability of the catalyst is still an important issue in practical applications. Undeniably, a lot more systematic explorations are still demanded to investigate the issue related to regeneration of AB.

Nonetheless, the development of new non-noble metal-based catalysts can help to further reveal the catalytic mechanism based on obtaining high performance. The study of catalytic mechanism can

provide guidance for the design of the efficient catalyst. The design and development of simulation calculation and in situ characterization testing technology is also very beneficial to the study of the structure and chemical state of the catalyst during the reaction process. We look forward to the further development of non-noble metal-based catalysts to meet the requirements of practical applications in the near future.

Acknowledgement

This work was supported by the National Natural Science Foundation of China (Nos. 51871088, 21603052, 51771068, and 51771067), the key Basic Research Programme of Hebei Province of China (17964401D), Natural Science Foundation of Tianjin (18JCQNJC77900), and the Natural Science Foundation of Hebei Province (Nos. B2019202194 and B201820167).

References

[1] Manoharan Y, Hosseini SE, Butler B, Alzhahrani H, Senior BTF, Ashuri T, Krohn J (2019) Hydrogen fuel cell vehicles; current status and future prospect. Appl Sci 9(11):2296

[2] Midilli A, Ay M, Dincer I, Rosen MA (2005) On hydrogen and hydrogen energy strategies. Renew Sustain Energy Rev 9(3):255–271

[3] Geng S, Yang W, Yu YS (2019) Building MoS2/S-doped g-C3N4 layered heterojunction electrocatalysts for efficient hydrogen evolution reaction. J Catal 375:441–447

[4] Hosseini SE, Wahid MA (2016) Hydrogen production from renewable and sustainable energy resources: Promising green energy carrier for clean development. Renew Sustain Energy Rev 57:850–866

[5] Møller KT, Jensen TR, Akiba E, Li HW (2017) Hydrogen-A sustainable energy carrier. Prog Nat Sci Mater Int 27(1):34–40

[6] He T, Pachfule P, Wu H, Xu Q, Chen P (2016) Hydrog carriers Nat Rev Mater 1(12):16067

[7] Yu X, Tang Z, Sun D, Ouyang L, Zhu M (2017) Recent advances and remaining challenges of nanostructured materials for hydrogen storage applications. Prog Mater Sci 88:1–48

[8] Bonaccorso F, Colombo L, Yu G, Stoller M, Tozzini V, Ferrari AC, Ruoff RS, Pellegrini V (2015) 2D materials Graphene related two-dimensional crystals and hybrid systems for energy conversion and storage. Science 347(6217):1246501

[9] Ren J, Musyoka NM, Langmi HW, Mathe M, Liao S (2017) Current research trends and perspectives on materials-based hydrogen storage solutions: A critical review. Int J Hydrog Energy 42(1):289–311

[10] Li L, Huang Y, An C, Wang Y (2019) Lightweight hydrides nanocomposites for hydrogen storage: Challenges, progress and prospects. Sci China Mater 62(11):1597–1625

[11] Kumar R, Karkamkar A, Bowden M, Autrey T (2019) Solid-state hydrogen rich boron-nitrogen compounds for energy storage. Chem Soc Rev 48(21):5350–5380

[12] Roy B, Hajari A, Kumar V, Manna J, Sharma P (2018) Kinetic model analysis and mechanistic correlation of ammonia borane thermolysis under dynamic heating conditions. Int J Hydrog Energy 43(22):10386–10395

[13] Sanyal U, Demirci UB, Jagirdar BR, Miele P (2011) Hydrolysis of ammonia borane as a hydrogen source: fundamental issues and potential solutions towards implementation. Chemsuschem 4(12):1731–1739

[14] Zhang H, Huang M, Wen J, Li Y, Li A, Zhang L, Ali AM, Li Y (2019) Sub-3 nm Rh nanoclusters confined within a metal-organic framework for enhanced hydrogen generation. Chem Commun (Camb) 55(32):4699–4702

[15] Yao K, Zhao C, Wang N, Li T, Lu W, Wang J (2020) An aqueous synthesis of porous PtPd nanoparticles with reversed bimetallic structures for highly efficient hydrogen generation from ammonia borane hydrolysis. Nanoscale 12(2):638–647

[16] Ma H, Na C (2015) Isokinetic temperature and size-controlled activation of ruthenium-catalyzed ammonia borane hydrolysis. ACS Catal 5(3):1726–1735

[17] Zhang L, Wang Y, Li J, Ren X, Lv H, Su X, Hu Y, Xu D, Liu B (2018) Ultrasmall Ru nanoclusters on nitrogen-enriched hierarchically porous carbon support as remarkably active catalysts for hydrolysis of ammonia borane. ChemCatChem 10(21):4910–4916

[18] Liu B, Xu Y, Zhang S, Lv X, Ling Y, Zhou Z, Liu J (2019) FeCo alloy encapsulated within carbon nanotube as efficient and stable catalyst for ammonia borane hydrolysis. Mater Lett 239:124–127

[19] Wang C, Tuninetti J, Wang Z, Zhang C, Ciganda R, Salmon L, Moya S, Ruiz J, Astruc D (2017) Hydrolysis of ammonia-borane over ni/zif-8 nanocatalyst: high efficiency, mechanism, and controlled hydrogen release. J Am Chem Soc 139(33):11610–11615

[20] Yüksel Alpaydın C, Gülbay SK, Ozgur Colpan C (2020) A review on the catalysts used for hydrogen production from ammonia borane. Int J Hydrog Energy 45(5):3414–3434

[21] WangFuYangMartinez MoroRamirezMoyaSalmonRuizAstruc QFSMMSLJD (2018) Dramatic synergy in copt nanocatalysts stabilized by "click" dendrimers for

evolution of hydrogen from hydrolysis of ammonia borane. ACS Catal 9(2):1110–1119

[22] Zhang J, Dong Y, Liu Q, Zhou M, Mi G, Du X (2019) Hierarchically alloyed Pd–Cu microarchitecture with tunable shapes: morphological engineering, and catalysis for hydrogen evolution reaction of ammonia borane. Int J Hydrog Energy 44(57):30226–30236

[23] Yang X, Cheng F, Liang J, Tao Z, Chen J (2011) Carbon-supported Ni1-x@Pt-x (x=0.32, 0.43, 0.60, 0.67, and 0.80) core-shell nanoparticles as catalysts for hydrogen generation from hydrolysis of ammonia borane. Int J Hydrog Energy 36(3):1984–1990

[24] Yang X, Cheng F, Tao Z, Chen J (2011) Hydrolytic dehydrogenation of ammonia borane catalyzed by carbon supported Co core-Pt shell nanoparticles. J Power Sour 196(5):2785–2789

[25] Yang X, Cheng F, Liang J, Tao Z, Chen J (2009) PtxNi1-x nanoparticles as catalysts for hydrogen generation from hydrolysis of ammonia borane. Int J Hydrog Energy 34(21):8785–8791

[26] Ren X, Lv H, Yang S, Wang Y, Li J, Wei R, Xu D, Liu B (2019) promoting effect of heterostructured nio/ni on pt nanocatalysts toward catalytic hydrolysis of ammonia borane. J Phys Chem Lett 10(23):7374–7382

[27] Kang K, Gu X, Guo L, Liu P, Sheng X, Wu Y, Cheng J, Su H (2015) Efficient catalytic hydrolytic dehydrogenation of ammonia borane over surfactant-free bimetallic nanoparticles immobilized on amine-functionalized carbon nanotubes. Int J Hydrog Energy 40(36):12315–12324

[28] Guo L, Gu X, Kang K, Wu Y, Cheng J, Liu P, Wang T, Su H (2015) Porous nitrogen-doped carbon-immobilized bimetallic nanoparticles as highly efficient catalysts for hydrogen generation from hydrolysis of ammonia borane. J Mater Chem A 3(45):22807–22815

[29] Liu M, Zhou L, Luo X, Wan C, Xu L (2020) Recent advances in noble metal catalysts for hydrogen production from ammonia borane. Catalysts 10(7):788

[30] Xu Q, Chandra M (2006) Catalytic activities of non-noble metals for hydrogen generation from aqueous ammonia-borane at room temperature. J Power Sources 163(1):364–370

[31] Chandra M, Xu Q (2006) A high-performance hydrogen generation system: Transition metal-catalyzed dissociation and hydrolysis of ammonia-borane. J Power Sour 156(2):190–194

[32] Nozaki A, Tanihara Y, Kuwahara Y, Ohmichi T, Mori K, Nagase T, Yasuda HY, Yamashita H (2016) Skeletal Ni catalysts prepared from amorphous Ni-Zr alloys: enhanced catalytic performance for hydrogen generation from ammonia borane. ChemPhysChem 17(3):412–417

[33] Nozaki A, Kittima S, Tanihara Y, Kuwahara Y, Ohmichi T, Kamegawa T, Mori K, Yamashita H (2016) Efficient hydrogen generation from ammonia borane on skeletal Cu catalysts prepared from Cu-Ti amorphous alloys. J Jpn Inst Met Mater 80(6):365–369

[34] Fang Y, Xiao Z, Li J, Lollar C, Liu L, Lian X, Yuan S, Banerjee S, Zhang P, Zhou HC (2018) Formation of a highly reactive cobalt nanocluster crystal within a highly negatively charged porous coordination cage. Angew Chem Int Ed 57(19):5283–5287

[35] Zhao X, Ke D, Han S, Li Y, Zhang H, Cai Y (2019a) Reduced graphene oxide sheets supported waxberry-like co catalysts for improved hydrolytic dehydrogenation of ammonia borane. ChemistrySelect 4(9):2513–2518

[36] Guo K, Li H, Yu Z (2018) Size-Dependent catalytic activity of monodispersed nickel nanoparticles for the hydrolytic dehydrogenation of ammonia borane. ACS Appl Mater Interfaces 10(1):517–525

[37] Wei W, Wang Z, Xu J, Zong L, Zhao K, Wang H, Li H, Yu R (2017) Cobalt hollow nanospheres: controlled synthesis, modification and highly catalytic performance for hydrolysis of ammonia borane. Sci Bull 62(5):326–331

[38] Li Z, He T, Liu L, Chen W, Zhang M, Wu G, Chen P (2017) Covalent triazine framework supported non-noble metal nanoparticles with superior activity for catalytic hydrolysis of ammonia borane: from mechanistic study to catalyst design. Chem Sci 8(1):781–788

[39] Zhang J, Chen C, Yan W, Duan F, Zhang B, Gao Z, Qin Y (2016) Ni nanoparticles supported on CNTs with excellent activity produced by atomic layer deposition for hydrogen generation from the hydrolysis of ammonia borane. Catal Sci Technol 6(7):2112–2119

[40] Zhang X-L, Zhang D-X, Chang G-G, Ma X-C, Wu J, Wang Y, Yu H-Z, Tian G, Chen J, Yang X-Y (2019) Bimetallic (Zn/Co) MOFs-derived highly dispersed metallic Co/HPC for completely hydrolytic dehydrogenation of Ammonia-Borane. Ind Eng Chem Res 58(17):7209–7216

[41] Zhang F, Ma C, Zhang Y, Li H, Fu D, Du X, Zhang X-M (2018) N-doped mesoporous carbon embedded Co nanoparticles for highly efficient and stable H-2 generation from hydrolysis of ammonia borane. J Power Sour 399:89–97

[42] Li M, Hu J, Lu H (2016) A stable and efficient 3D cobalt-graphene composite catalyst for the hydrolysis of ammonia borane. Catal Sci Technol 6(19):7186–7192

[43] Wen M, Cui Y, Kuwahara Y, Mori K, Yamashita H (2016) Non-noble-metal nanoparticle supported on metal-organic framework as an efficient and durable catalyst for promoting h-2 production from ammonia borane under visible light irradiation. ACS Appl Mater Inter 8(33):21278–21284

[44] Song J, Gu X, Cheng J, Fan N, Zhang H, Su H (2018) Remarkably boosting catalytic H-2 evolution from ammonia borane through the visible-light-driven synergistic electron effect of non-plasmonic noble-metal-free nanoparticles and photoactive metal-organic frameworks. Appl Catal 225:424–432

[45] Liu P, Gu X, Kang K, Zhang H, Cheng J, Su H (2017) Highly efficient catalytic hydrogen evolution from ammonia borane using the synergistic effect of crystallinity and size of noble-metal-free nanoparticles supported by porous metal organic frameworks. ACS Appl Mater Inter 9(12):10759–10767

[46] Liu H, Liu X, Yang W, Shen M, Geng S, Yu C, Shen B, Yu Y (2019) Photocatalytic dehydrogenation of formic acid promoted by a superior PdAg@g-C3N4 Mott-Schottky heterojunction. J Mater Chem A 7(5):2022–2026

[47] Wang C, Sun D, Yu X, Zhang X, Lu Z, Wang X, Zhao J, Li L, Yang X (2018) Cu/Ni nanoparticles supported on TiO2(B) nanotubes as hydrogen generation photocatalysts via hydrolysis of ammonia borane. Inorg Chem Front 5(8):2038–2044

[48] Wang C, Yu X, Zhang X, Lu Z, Wang X, Han X, Zhao J, Li L, Yang X (2020) Enhanced hydrogen production from ammonia borane over CuNi alloy nanoparticles supported on TiO2(B)/anatase mixed-phase nanofibers with high specific surface area. J Alloys Compd 815:152431

[49] Wang Y, Bao S, Liu Y, Yang W, Yu Y, Feng M, Li K (2020) Efficient photocatalytic reduction of Cr(VI) in aqueous solution over CoS2/g-C3N4-rGO nanocomposites under visible light. Appl Surf Sci 510:145495

[50] Zhang H, Gu X, Song J, Fan N, Su H (2017) Non-Noble metal nanoparticles supported by postmodified porous organic semiconductors: highly efficient catalysts for visible-light-driven on-demand H-2 evolution from ammonia borane. ACS Appl Mater Inter 9(38):32767–32774

[51] Song J, Gu X, Cao Y, Zhang H (2019) Porous oxygen vacancy-rich V2O5 nanosheets as superior semiconducting supports of nonprecious metal nanoparticles for efficient on-demand H2 evolution from ammonia borane under visible light irradiation. J Mater Chem A 7(17):10543–10551

[52] Zhang H, Gu X, Song J (2020) Co, Ni-based nanoparticles supported on graphitic carbon nitride nanosheets as catalysts for hydrogen generation from the hydrolysis of ammonia borane under broad-spectrum light irradiation. Int J Hydrog Energy 45(41):21273–21286

[53] Yan J-M, Zhang X-B, Han S, Shioyama H, Xu Q (2009) Magnetically recyclable Fe-Ni alloy catalyzed dehydrogenation of ammonia borane in aqueous solution under ambient atmosphere. J Power Sour 194(1):478–481

[54] Yang K, Yao QL, Lu ZH, Kang ZB, Chen XS (2017) Facile synthesis of cumo nanoparticles as highly active and cost-effective catalysts for the hydrolysis of ammonia borane. Acta Phys-Chim Sin 33(5):993–1000

[55] Yang K, Yao Q, Huang W, Chen X, Lu Z-H (2017) Enhanced catalytic activity of NiM (M=Cr, Mo, W) nanoparticles for hydrogen evolution from ammonia borane and hydrazine borane. Int J Hydrog Energy 42(10):6840–6850

[56] Furukawa S, Nishimura G, Takayama T, Komatsu T (2019) Highly Active Ni- and Co-Based Bimetallic Catalysts for Hydrogen Production From Ammonia-Borane. Front Chem 7:138

[57] Zhang J, Li H, Zhang H, Zhu Y, Mi G (2016) Porously hierarchical Cu@Ni cubic-cage microstructure: Very active and durable catalyst for hydrolytically liberating H-2 gas from ammonia borane. Renew Energy 99:1038–1045

[58] Wang C, Li L, Yu X, Lu Z, Zhang X, Wang X, Yang X, Zhao J (2020) Regulation of d-Band Electrons to Enhance the Activity of Co-Based Non-Noble Bimetal Catalysts for Hydrolysis of Ammonia Borane. ACS Sustainable Chem Eng 8(22):8256–8266

[59] Wang C, Wang H, Wang Z, Li X, Chi Y, Wang M, Gao D, Zhao Z (2018) Mo remarkably enhances catalytic activity of Cu@MoCo core-shell nanoparticles for hydrolytic dehydrogenation of ammonia borane. Int J Hydrog Energy 43(15):7347–7355

[60] Sang W, Wang C, Zhang X, Yu X, Yu C, Zhao J, Wang X, Yang X, Li L (2017) Dendritic Co0.52Cu0.48 and Ni0.19Cu0.81 alloys as hydrogen generation catalysts via hydrolysis of ammonia borane. Int J Hydrog Energy 42(52):30691–30703

[61] Li S-J, Wang H-L, Yan J-M, Jiang Q (2017) Oleylamine-stabilized Cu0.9Ni0.1 nanoparticles as efficient catalyst for ammonia borane dehydrogenation. Int J Hydrog Energy 42(40):25251–25257

[62] Bulut A, Yurderi M, Ertas IE, Celebi M, Kaya M, Zahmakiran M (2016) Carbon dispersed copper-cobalt alloy nanoparticles: a cost-effective heterogeneous catalyst with exceptional performance in the hydrolytic dehydrogenation of ammonia-borane. Appl Catal B 180:121–129

[63] Sun D, Hao Y, Wang C, Zhang X, Yu X, Yang X, Li L, Lu Z, Shang W (2020) TiO2-CdS supported CuNi nanoparticles as a highly efficient catalyst for hydrolysis of ammonia borane under visible-light irradiation. Int J Hydrog Energy 45(7):4390–4402

[64] Yang X, Li Q, Li L, Lin J, Yang X, Yu C, Liu Z, Fang Y, Huang Y, Tang C (2019) CuCo binary metal nanoparticles supported on boron nitride nanofibers as highly efficient catalysts for hydrogen generation from hydrolysis of ammonia borane. J Power Sour 431:135–143

[65] Zacho SL, Mielby J, Kegnaes S (2018) Hydrolytic dehydrogenation of ammonia borane over ZIF-67 derived Co nanoparticle catalysts. Catal Sci Technol 8(18):4741–4746

[66] Wang H, Zhao Y, Cheng F, Tao Z, Chen J (2016) Cobalt nanoparticles embedded in porous N-doped carbon as long-life catalysts for hydrolysis of ammonia borane. Catal Sci Technol 6(10):3443–3448

[67] Lee M-H, Deka JR, Cheng C-J, Lu N-F, Saikia D, Yang Y-C, Kao H-M (2019) Synthesis of highly dispersed ultra-small cobalt nanoparticles within the cage-type mesopores of 3D cubic mesoporous silica via double agent reduction method for catalytic hydrogen generation. Appl Surf Sci 470:764–772

[68] Gao M, Yu Y, Yang W, Li J, Xu S, Feng M, Li H (2019) Ni nanoparticles supported on graphitic carbon nitride as visible light catalysts for hydrolytic dehydrogenation of ammonia borane. Nanoscale 11(8):3506–3513

[69] Wu Y, Wu X, Liu Q, Huang C, Qiu X (2017) Magnetically recyclable Ni@h-BN composites for efficient hydrolysis of ammonia borane. Int J Hydrogen Energy 42(25):16003–16011

[70] Yang XJ, Li LL, Sang WL, Zhao JL, Wang XX, Yu C, Zhang XH, Tang CC (2017) Boron nitride supported Ni nanoparticles as catalysts for hydrogen generation from hydrolysis of ammonia borane. J Alloys Compd 693:642–649

[71] Qiu X, Wu X, Wu Y, Liu Q, Huang C (2016) The release of hydrogen from ammonia borane over copper/hexagonal boron nitride composites. RSC Adv 6(108):106211–106217

[72] Al-Enizil AM, Brooks RM, Ahmad MM, Ei-Halwany MM, El-Newehy MH, Yousef A (2018) In-situ synthesis of amorphous co nanoparticles supported onto TiO2 nanofibers as a catalyst for hydrogen generation from the hydrolysis of ammonia borane. J Nanosci Nanotechnol 18(7):4714–4719

[73] Zhu J, Ma L, Feng J, Geng T, Wei W, Xie J (2018) Facile synthesis of Cu nanoparticles on different morphology ZrO2 supports for catalytic hydrogen generation from ammonia borane. J Mater Sci Mater Electron 29(17):14971–14980

[74] Liu T, Wang Q-T, Sun Y-H, Zhao M (2019) Facile synthesis of monodispersed co nanoparticles on titanium carbides for hydrolysis of ammonia borane at mild temperature. J Nanosci Nanotechnol 19(11):7392–7397

[75] Chen M, Xiong R, Cui X, Wang Q, Liu X (2019) SiO2-encompassed Co@N-doped porous carbon assemblies as recyclable catalysts for efficient hydrolysis of ammonia borane. Langmuir 35(3):671–677

[76] Li YT, Ullah S, Han Z, Zheng XC, Zheng GP (2020) Hierarchical porous CuNi-based bimetal-organic frameworks as efficient catalysts for ammonia borane hydrolysis. Catal Commun 143:106057

[77] Chen MJ, Zhang DX, Li D, Ke SC, Ma XC, Chang GG, Chen J, Yang XY (2020) All-around coating of CoNi nanoalloy using a hierarchically porous carbon derived from bimetallic MOFs for highly efficient hydrolytic dehydrogenation of ammonia-borane. New J Chem 44(7):3021–3027

[78] Cui C, Liu Y, Mehdi S, Wen H, Zhou B, Li J, Li B (2020) Enhancing effect of Fe-doping on the activity of nano Ni catalyst towards hydrogen evolution from NH3BH3. Appl Catal B. https://doi.org/10.1016/j.apcatb.2020.118612

[79] Zhao X, Ke D, Han S, Li Y, Zhang H, Cai Y (2019b) Surfactant PVA-stabilized Co-Mo nanocatalyst supported by graphene oxide sheets toward the hydrolytic dehydrogenation of ammonia borane. NANO 14(11):1950137

[80] Brooks RM, Maafa IM, Al-Enizi AM, El-Halwany MM, Ubaidullah M, Yousef A (2019) Electrospun bimetallic nicr nanoparticles@carbon nanofibers as an efficient catalyst for hydrogen generation from ammonia borane. Nanomaterials 9(8):1082

[81] Xu M, Huai X, Zhang H (2018) Highly dispersed CuCo nanoparticles supported on reduced graphene oxide as high-activity catalysts for hydrogen evolution from ammonia borane hydrolysis. J Nanopart Res 20(12):329

[82] Du X, Tai Y, Liu H, Zhang J (2018) One-step synthesis of reduced graphene oxide supported CoW nanoparticles as efficient catalysts for hydrogen generation from NH3BH3. React Kinet Mech Catal 125(1):171–181

[83] Wang Q, Zhang F, Du F, Liu T (2017) A cost effective cobalt nickel nanoparticles catalyst with exceptional performance for hydrolysis of ammonia-borane. J Nanosci Nanotechnol 17(12):9333–9338

[84] Wang Q, Zhang Z, Liu J, Liu R, Liu T (2018) Bimetallic non-noble CoNi nanoparticles monodispersed on multiwall carbon nanotubes: highly efficient hydrolysis of ammonia borane. Mater Chem Phys 204:58–61

[85] Song F-Z, Zhu Q-L, Yang X-C, Xu Q (2016) Monodispersed CuCo nanoparticles supported on diamine-functionalized graphene as a non-noble metal catalyst for hydrolytic dehydrogenation of ammonia borane. Chemnanomat 2(10):942–945

[86] Yao Q, Lu Z-H, Huang W, Chen X, Zhu J (2016) High Pt-like activity of the Ni-Mo/graphene catalyst for hydrogen evolution from hydrolysis of ammonia borane. J Mater Chem A 4(22):8579–8583

[87] Zhao B, Liu J, Zhou L, Long D, Feng K, Sun X, Zhong J (2016) Probing the electronic structure of M-graphene oxide (M=Ni Co, NiCo) catalysts for hydrolytic dehydrogenation of ammonia borane. Appl Surf Sci 362:79–85

[88] Liang Z, Xiao X, Yu X, Huang X, Jiang Y, Fan X, Chen L (2018) Non-noble trimetallic Cu-Ni-Co nanoparticles supported on metal-organic frameworks as highly efficient catalysts for hydrolysis of ammonia borane. J Alloys Compd 741:501–508

[89] Zhang H, Gu X, Liu P, Song J, Cheng J, Su H (2017) Highly efficient visible-light-driven catalytic hydrogen evolution from ammonia borane using non-precious metal nanoparticles supported by graphitic carbon nitride. J Mater Chem A 5(5):2288–2296

[90] Cheng S, Liu Y, Zhao Y, Zhao X, Lang Z, Tan H, Qiu T, Wang Y (2019) Superfine CoNi alloy embedded in Al2O3 nanosheets for efficient tandem catalytic reduction of nitroaromatic compounds by ammonia borane. Dalton Trans 48(47):17499–17506

[91] Guo K, Ding Y, Luo J, Gu M, Yu Z (2019) NiCu bimetallic nanoparticles on silica support for catalytic hydrolysis of ammonia borane: composition-dependent activity and support size effect. ACS Appl Energy Mater 2(8):5851–5861

[92] Liao J, Lv F, Feng Y, Zhong S, Wu X, Zhang X, Wang H, Li J, Li H (2019) Electromagnetic-field-assisted synthesis of Ni foam film-supported CoCu alloy microspheres composed of nanosheets: a high performance catalyst for the hydrolysis of ammonia borane. Catal Commun 122:16–19

[93] Liu Y, Zhang J, Guan H, Zhao Y, Yang J-H, Zhang B (2018) Preparation of bimetallic Cu-Co nanocatalysts on poly (diallyldimethylammonium chloride) functionalized halloysite nanotubes for hydrolytic dehydrogenation of ammonia borane. Appl Surf Sci 427:106–113

[94] Fan D, Lv X, Feng J, Zhang S, Bai J, Lu R, Liu J (2017) Cobalt nickel nanoparticles encapsulated within hexagonal boron nitride as stable, catalytic dehydrogenation nanoreactor. Int J Hydrog Energy 42(16):11312–11320

[95] Brown HSH, Finholt A, Gilbreath J, Hoekstra H, Hyde E (1953) Sodium borohydride its hydrolysis and its use as a reducing agent and in the generation of hydrogen. J Am Chem Soc 75(1):215–219

[96] Wang X, Liao J, Li H, Wang H, Wang R (2016) Solid-state-reaction synthesis of cotton-like CoB alloy at room temperature as a catalyst for hydrogen generation. J Colloid Interface Sci 475:149–153

[97] Wang Y, Meng W, Wang D, Li G, Wu S, Cao Z, Zhang K, Wu C, Liu S (2017) Nanostructured thin-film Co-B catalysts for hydrogen generation from hydrolysis of ammonia borane. Int J Hydrog Energy 42(52):30718–30726

[98] Zou Y, Gao Y, Xiang C, Chu H, Qiu S, Yan E, Xu F, Tang C, Sun L (2016) Cobalt-nickel-boron supported over polypyrrole-derived activated carbon for hydrolysis of ammonia borane. Metals 6(7):154

[99] Li C, Wang D, Wang Y, Li G, Hu G, Wu S, Cao Z, Zhang K (2018) Enhanced catalytic activity of the nanostructured Co-W-B film catalysts for hydrogen evolution from the hydrolysis of ammonia borane. J Colloid Interface Sci 524:25–31

[100] Li C, Meng W, Hu G, Wang Y, Cao Z, Zhang K (2018) Preparation and characterization of nanostructured Co-Mo-B thin film catalysts for the hydrolysis of ammonia borane. Int J Hydrog Energy 43(37):17664–17672

[101] Wang Y, Meng W, Wang D, Wang Z, Zou K, Cao Z, Zhang K, Wu S, Li G (2019) Ultrafine cobalt-molybdenum-boron nanocatalyst for enhanced hydrogen generation property from the hydrolysis of ammonia borane. Int J Hydrog Energy 44(41):23267–23276

[102] Wang Y, Wang D, Zhao C, Meng W, Zhao T, Cao Z, Zhang K, Bai S, Li G (2019) Co-Mo-B nanoparticles supported on foam Ni as efficient catalysts for hydrogen generation from hydrolysis of ammonia borane solution. Int J Hydrog Energy 44(21):10508–10518

[103] Men Y, Su J, Du X, Liang L, Cheng G, Luo W (2018) CoBP nanoparticles supported on three-dimensional nitrogen-doped graphene hydrogel and their superior catalysis for hydrogen generation from hydrolysis of ammonia borane. J Alloys Compd 735:1271–1276

[104] Cui L, Xu Y, Niu L, Yang W, Liu J (2017) Monolithically integrated CoP nanowire array: An on/off switch for effective on-demand hydrogen generation via hydrolysis of NaBH4 and NH3BH3. Nano Res 10(2):595–604

[105] Tang C, Qu F, Asiri AM, Luo Y, Sun X (2017) CoP nanoarray: a robust non-noble-metal hydrogen-generating catalyst toward effective hydrolysis of ammonia borane. Inorg Chem Front 4(4):659–662

[106] Tang C, Xie L, Wang K, Du G, Asiri AM, Luo Y, Sun X (2016) A Ni2P nanosheet array integrated on 3D Ni foam: an efficient, robust and reusable monolithic catalyst for the hydrolytic dehydrogenation of ammonia borane toward on-demand hydrogen generation. J Mater Chem A 4(32):12407–12410

[107] Qu X, Jiang R, Li Q, Zeng F, Zheng X, Xu Z, Chen C, Peng J (2019) The hydrolysis of ammonia borane catalyzed by NiCoP/OPC-300 nanocatalysts: high selectivity and efficiency, and mechanism. Green Chem 21(4):850–860

[108] Fu Z-C, Xu Y, Chan SL-F, Wang W-W, Li F, Liang F, Chen Y, Lin Z-S, Fu W-F, Che C-M (2017) Highly efficient hydrolysis of ammonia borane by anion (-OH, F-, Cl-)-tuned interactions between reactant molecules and CoP nanoparticles. Chem Commun 53(4):705–708

[109] Hou C-C, Li Q, Wang C-J, Peng C-Y, Chen Q-Q, Ye H-F, Fu W-F, Che C-M, Lopez N, Chen Y (2017) Ternary Ni-Co-P nanoparticles as noble-metal-free catalysts to boost

the hydrolytic dehydrogenation of ammonia-borane. Energy Environ Sci 10(8):1770–1776

[110] Wang Y, Shen G, Zhang Y, Pan L, Zhang X, Zou J-J (2020) Visible-light-induced unbalanced charge on NiCoP/TiO2 sensitized system for rapid H-2 generation from hydrolysis of ammonia borane. Appl Catal B 260:118183

[111] Kalidindi SB, Sanyal U, Jagirdar BR (2008) Nanostructured Cu and Cu@Cu(2)O core shell catalysts for hydrogen generation from ammonia-borane. Phys Chem Chem Phys 10(38):5870–5874

[112] Filiz BC, Figen AK, Piskin S (2018) Dual combining transition metal hybrid nanoparticles for ammonia borane hydrolytic dehydrogenation. Appl Catal A 550:320–330

[113] Feng X, Chen X-M, Qiu P, Wu D, Hamilton EJM, Zhang J, Chen X (2018) Copper oxide hollow spheres: Synthesis and catalytic application in hydrolytic dehydrogenation of ammonia borane. Int J Hydrog Energy 43(45):20875–20881

[114] Komova OV, Odegova GV, Gorlova AM, Bulavchenko OA, Pochtar AA, Netskina OV, Simagina VI (2019) Copper-iron mixed oxide catalyst precursors prepared by glycine-nitrate combustion method for ammonia borane dehydrogenation processes. Int J Hydrog Energy 44(44):24277–24291

[115] Liu Y, Guo H, Sun K, Jiang J (2019) Magnetic CoOx@C-reduced graphene oxide composite with catalytic activity towards hydrogen generation. Int J Hydrog Energy 44(52):28163–28172

[116] Liao J, Feng Y, Lin W, Su X, Ji S, Li L, Zhang W, Pollet BG, Li H (2020) CuO-NiO/Co3O4 hybrid nanoplates as highly active catalyst for ammonia borane hydrolysis. Int J Hydrog Energy 45(15):8168–8176

[117] Feng Y, Wang H, Chen X, Lv F, Li Y, Zhu Y, Xu C, Zhang X, Liu H-R, Li H (2020) Simple synthesis of Cu2O–CoO nanoplates with enhanced catalytic activity for hydrogen production from ammonia borane hydrolysis. Int J Hydrog Energy 45(35):17164–17173

[118] Guan SY, An LL, Ashraf S, Zhang LN, Liu BZ, Fan YP, Li BJ (2020a) Oxygen vacancy excites Co3O4 nanocrystals embedded into carbon nitride for accelerated hydrogen generation. Appl Catal B 269:118775

[119] Li X, Gui L, Zou H (2019) Bracelet-like Ni04Cu06O microstructure composed of well-aligned nanoplatelets as a superior catalyst to the hydrolysis of ammonia borane. Front Chem 7:776

[120] Feng K, Zhong J, Zhao B, Zhang H, Xu L, Sun X, Lee S-T (2016) CuxCo1-xO nanoparticles on graphene oxide as a synergistic catalyst for high-efficiency hydrolysis of ammonia-borane. Angew Chem Int Ed 55(39):11950–11954

[121] Zheng H, Feng K, Shang Y, Kang Z, Sun X, Zhong J (2018) Cube-like CuCoO nanostructures on reduced graphene oxide for H-2 generation from ammonia borane. Inorg Chem Front 5(5):1180–1187

[122] Shang Y, Feng K, Wang Y, Sun X, Zhong J (2019) Carbon nitride supported Ni0.5Co0.5O nanoparticles with strong interfacial interaction to enhance the hydrolysis of ammonia borane. RSC Adv 9(20):11552–11557

[123] Guo X, Li M, Liu Y, Huang Y, Geng S, Yang W, Yu Y (2020) Hierarchical core-shell electrode with NiWO4 nanoparticles wrapped MnCo2O4 nanowire arrays on Ni foam for high-performance asymmetric supercapacitors. J Colloid Interface Sci 563:405–413

[124] Liao J, Feng Y, Wu S, Ye H, Zhang J, Zhang X, Xie F, Li H (2019) Hexagonal CuCo2O4 nanoplatelets, a highly active catalyst for the hydrolysis of ammonia borane for hydrogen production. Nanomaterials 9(3):360

[125] Liu Q, Zhang S, Liao J, Feng K, Zheng Y, Pollet BG, Li H (2017) CuCo2O4 nanoplate film as a low-cost, highly active and durable catalyst towards the hydrolytic dehydrogenation of ammonia borane for hydrogen production. J Power Sour 355:191–198

[126] Liu Q, Zhang S, Liao J, Huang X, Zheng Y, Li H (2017) MnCo2O4 film composed of nanoplates: synthesis, characterization and its superior catalytic performance in the hydrolytic dehydrogenation of ammonia borane. Catal Sci Technol 7(16):3573–3579

[127] Liao J, Li H, Zhang X, Feng K, Yao Y (2016) Fabrication of a Ti-supported NiCo2O4 nanosheet array and its superior catalytic performance in the hydrolysis of ammonia borane for hydrogen generation. Catal Sci Technol 6(11):3893–3899

[128] Lu D, Liao J, Zhong S, Leng Y, Ji S, Wang H, Wang R, Li H (2018) Cu06Ni04Co2O4 nanowires, a novel noble-metal free catalyst with ultrahigh catalytic activity towards the hydrolysis of ammonia borane for hydrogen production. Int J Hydrog Energy 43(11):5541–5550

[129] Lu D, Li J, Lin C, Liao J, Feng Y, Ding Z, Li Z, Liu Q, Li H (2019) A simple and scalable route to synthesize CoxCu1-xCo2O4@CoyCu1-yCo2O4 yolk-shell microspheres, a high-performance catalyst to hydrolyze ammonia borane for hydrogen production. Small 15(10):1805460

[130] Feng Y, Zhang J, Ye H, Li L, Wang H, Li X, Zhang X, Li H (2019) Ni05Cu05Co2O4 nanocomposites, morphology, controlled synthesis, and catalytic performance in the hydrolysis of ammonia borane for hydrogen production. Nanomaterials 9(9):1334

[131] Lu D, Liao J, Li H, Ji S, Pollet BG (2019) Co3O4/CuMoO4 hybrid microflowers composed of nanorods with rich particle boundaries as a highly active catalyst for ammonia

borane hydrolysis. ACS Sustain Chem Eng 7(19):16474–16482

[132] Lu D, Liao J, Leng Y, Zhong S, He J, Wang H, Wang R, Li H (2018) Mo-doped Cu0.5Ni0.5Co2O4 nanowires, a strong substitute for noble-metal-based catalysts towards the hydrolysis of ammonia borane for hydrogen production. Catal Commun 114:89–92

[133] Lu D, Feng Y, Ding Z, Liao J, Zhang X, Liu H-R, Li H (2019) MoO3-doped MnCo2O4 microspheres consisting of nanosheets: an inexpensive nanostructured catalyst to hydrolyze ammonia borane for hydrogen generation. Nanomaterials 9(1):21

[134] Liao J, Lu D, Diao G, Zhang X, Zhao M, Li H (2018) Co0.8Cu0.2MoO4 microspheres composed of nanoplatelets as a robust catalyst for the hydrolysis of ammonia borane. ACS Sustain Chem Eng 6(5):5843–5851

[135] Li J, Li F, Liao J, Liu Q, Li H (2019) Cu0.4Co0.6MO4 nanorods supported on graphitic carbon nitride as a highly active catalyst for the hydrolytic dehydrogenation of ammonia borane. Catalysts 9(9):714

[136] Yin H, Kuwahara Y, Mori K, Cheng H, Wen M, Huo Y, Yamashita H (2017) Localized surface plasmon resonances in plasmonic molybdenum tungsten oxide hybrid for visible-light-enhanced catalytic reaction. J Phys Chem C 121(42):23531–23540

[137] Yin H, Kuwahara Y, Mori K, Cheng H, Wen M, Yamashita H (2017) High-surface-area plasmonic MoO3-x: rational synthesis and enhanced ammonia borane dehydrogenation activity. J Mater Chem A 5(19):8946–8953

[138] Gong J, Li Z, Zhang T, Chen R, Zheng X, Zhang G (2017) Morphology-dependent catalytic activity of plasmonic MoO3-x for hydrolytic dehydrogenation of ammonia borane. Funct Mater Lett 10(6):1750079

[139] Yousef A, Brooks RM, El-Halwany MM, Obaid M, El-Newehy MH, Al-Deyab SS, Barakat NAM (2016) A novel and chemical stable Co-B nanoflakes-like structure supported over titanium dioxide nanofibers used as catalyst for hydrogen generation from ammonia borane complex. Int J Hydrog Energy 41(1):285–293

[140] Izgi MS, Sahin O, Saka C (2019) gamma-Al2O3 supported/Co-Cr-B catalyst for hydrogen evolution via NH3BH3 hydrolysis. Mater Manuf Processes 34(14):1620–1626

[141] Wang Y, Zou KL, Wang D, Meng W, Qi N, Cao ZQ, Zhang K, Chen HH, Li GD (2020) Highly efficient hydrogen evolution from the hydrolysis of ammonia borane solution with the Co-Mo-B/NF nanocatalyst. Renew Energy 154:453–460

[142] Feng X, Zhao Y, Liu D, Mo Y, Liu Y, Chen X, Yan W, Jin X, Chen B, Duan X, Chen D, Yang C (2018) Towards high activity of hydrogen production from ammonia borane over efficient non-noble Ni5P4 catalyst. Int J Hydrog Energy 43(36):17112–17120

[143] Du X, Yang C, Zeng X, Wu T, Zhou Y, Cai P, Cheng G, Luo W (2017) Amorphous NiP supported on rGO for superior hydrogen generation from hydrolysis of ammonia borane. Int J Hydrog Energy 42(20):14181–14187

[144] Zhang R, Zheng J, Chen T, Ma G, Zhou W (2018) RGO-wrapped Ni-P hollow octahedrons as noble-metal-free catalysts to boost the hydrolysis of ammonia borane toward hydrogen generation. J Alloys Compd 763:538–545

[145] Hou C-C, Chen Q-Q, Li K, Wang C-J, Peng C-Y, Shi R, Chen Y (2019) Tailoring three-dimensional porous cobalt phosphides templated from bimetallic metal-organic frameworks as precious metal-free catalysts towards the dehydrogenation of ammonia-borane. J Mater Chem A 7(14):8277–8283

[146] Du Y, Liu C, Cheng G, Luo W (2017) Cuboid Ni2P as a bifunctional catalyst for efficient hydrogen generation from hydrolysis of ammonia borane and electrocatalytic hydrogen evolution. Chem-Asian J 12(22):2967–2972

[147] Ma X-C, He Y-Y, Zhang D-X, Chen M-J, Ke S-C, Yin Y-X, Chang G-G (2020) Cobalt-based MOF-derived CoP/Hierarchical porous carbon (HPC) composites as robust catalyst for efficient dehydrogenation of ammonia-borane. Chemistryselect 5(7):2190–2196

[148] Oh S, Song D, Kim H, Sohn D, Hong K, Lee M, Son S, Cho E, Kwon H (2019) Cobalt-iron-phosphorus catalysts for efficient hydrogen generation from hydrolysis of ammonia borane solution. J Alloys Compd 806:643–649

[149] Yang J, Yuan Q, Liu Y, Huang X, Qiao Y, Lu J, Song C (2019) Low-cost ternary Ni-Fe-P catalysts supported on Ni foam for hydrolysis of ammonia borane. Inorg Chem Front 6(5):1189–1194

[150] Yang C, Men Y, Xu Y, Liang L, Cai P, Luo W (2019) In Situ Synthesis of NiCoP nanoparticles supported on reduced graphene oxide for the catalytic hydrolysis of ammonia borane. ChemPlusChem 84(4):382–386

[151] Zhou X, Meng X-F, Wang J-M, Shang N-Z, Feng T, Gao Z-Y, Zhang H-X, Ding X-L, Gao S-T, Feng C, Wang C (2019) Boron nitride supported NiCoP nanoparticles as noble metal-free catalyst for highly efficient hydrogen generation from ammonia borane. Int J Hydrog Energy 44(10):4764–4770

[152] Lin Y, Yang L, Jiang H, Zhang Y, Cao D, Wu C, Zhang G, Jiang J, Song L (2019) Boosted reactivity of ammonia borane dehydrogenation over Ni/Ni2P heterostructure. J Phys Chem Lett 10(5):1048–1054

[153] Li J, Ren X, Lv H, Wang Y, Li Y, Liu B (2020) Highly efficient hydrogen production from hydrolysis of ammonia

borane over nanostructured Cu@CuCoOx supported on graphene oxide. J Hazard Mater 391:122199–122199

[154] Zhang H, Fan Y, Liu B, Liu Y, Ashraf S, Wu X, Han G, Gao J, Li B (2019) Birdcage-type CoOx-carbon catalyst derived from metal-organic frameworks for enhanced hydrogen generation. ACS Sustain Chem Eng 7(11):9782–9792

[155] Du J, Hou J, Li B, Qin R, Xu C, Liu H (2020) Support-free 3D hierarchical nanoporous Cu@Cu2O for fast tandem ammonia borane dehydrogenation and nitroarenes hydrogenation under mild conditions. J Alloys Compd 815:152372

[156] Yao Q, Lu Z-H, Yang Y, Chen Y, Chen X, Jiang H-L (2018) Facile synthesis of graphene-supported Ni-CeOx nanocomposites as highly efficient catalysts for hydrolytic dehydrogenation of ammonia borane. Nano Res 11(8):4412–4422

[157] Men Y, Su J, Huang C, Liang L, Cai P, Cheng G, Luo W (2018) Three-dimensional nitrogen-doped graphene hydrogel supported Co-CeOx nanoclusters as efficient catalysts for hydrogen generation from hydrolysis of ammonia borane. Chin Chem Lett 29(11):1671–1674

[158] Hu J, Chen Z, Li M, Zhou X, Lu H (2014) Amine-capped Co nanoparticles for highly efficient dehydrogenation of ammonia borane. ACS Appl Mater Inter 6(15):13191–13200

[159] Peng CY, Kang L, Cao S, Chen Y, Lin ZS, Fu WF (2015) Nanostructured Ni2 P as a robust catalyst for the hydrolytic dehydrogenation of ammonia-borane. Angew Chem Int Ed Engl 54(52):15725–15729

[160] Guan S, An L, Ashraf S, Zhang L, Liu B, Fan Y, Li B (2020b) Oxygen vacancy excites Co3O4 nanocrystals embedded into carbon nitride for accelerated hydrogen generation. Appl Catal B 269:118775

[161] Ramachandran PV, Raju BC, Gagare PD (2012) One-pot synthesis of ammonia-borane and trialkylamine-boranes from trimethyl borate. Org Lett 14(24):6119–6121

[162] Liu C-H, Wu Y-C, Chou C-C, Chen B-H, Hsueh C-L, Ku J-R, Tsau F (2012) Hydrogen generated from hydrolysis of ammonia borane using cobalt and ruthenium based catalysts. Int J Hydrog Energy 37(3):2950–2959